Abstract

The concept of run-off triangles is widely used within the actuarial field. Its purpose is to estimate Incurred But Not Reported claims for insurance portfolios, in order to set appropriate reserves that are in compliance with regulatory requirements as well as the company's risk appetite. In this thesis, a parametric approach is proposed, where the portfolios are modeled using non-stationary distributions. The non-stationarity is able to account for various dependencies arising within the run-off triangle. In order to handle negative values, the families within the Generalized Extreme Value distribution have been applied. The findings are then benchmarked by comparing the method to a non-parametric Chain Ladder bootstrap approach. Using Value-at-Risk and Tail Value-at-Risk measures, the aggregated reserve is then estimated through Monte Carlo simulations by applying elliptical copulas, where the effects from dependence between portfolios are studied. The method is applied on data provided by a Swedish reinsurer, for its portfolios Aviation, Marine and Property. The implementation of the method conveys the impact of model risk and the importance of accurate parameter estimation, otherwise resulting in unrealistic projections. Additionally, dependence for different copulas, tail dependence in particular, is proven to have considerable effect for aggregated loss reserving.

Keywords: Run-off triangle, IBNR, Non-stationary marginal distributions, Elliptical copulas, Generalized Extreme Value distribution, Value at Risk, Maximum Likelihood Estimation, Chain Ladder.

Acknowledgements

We would like to thank our supervisor Nader Tajvidi at Faculty of Engineering, Lund University, for the support and contribution to this thesis. We are also very grateful to Lasse Klingberg, Chief Actuary, and his colleagues at Sirius International who have given us a lot of valuable inputs and provided us with the data used during the project.

Contents

Chapter 1

1 Introduction

1.1 Background

A fundamental aspect of the insurance industry is the management of loss reserves that cover for future payments arising from incurred claims. The amount of reserves an insurer should hold is a delicate matter. Too low reserves risk leaving the company in financial distress or bankruptcy, while too high reserves will lower profitability and thus the company's competitiveness in the market. The underlying driver for estimating reserves is the estimation of future payments from cedents' claims, i.e. Incurred But Not Reported (IBNR) claims. As a consequence, estimating IBNR is crucial for setting appropriate loss reserve amounts.

When predicting future claims, they are generally estimated seperately for the insurer's different portfolios, or lines of business (LoBs), which are typically categorized by the type of insurance, e.g. Accident & Health, Automotive, Property etc.. A classical framework that visualizes historical payments from a single LoB involves illustration in a triangular manner, which allows practitioners to track the time development of payments. Future claims are then estimated based on the triangular framework, known as a run-off triangle. There exists a substantial amount of actuarial theory on loss reserving using run-off triangles. The most fundamental, simplistic and most recognized methods are the Chain Ladder method and the Bornhuetter-Ferguson method[1].

The loss reserves from each individual LoB are combined in order to estimate an aggregated reserve for the insurer or reinsurer. As is well known, the risk of the aggregated loss reserve will be less than the sum of the risk for each LoB, since insurance portfolios are not perfectly correlated. There-

fore, diversification effects have a considerable impact on the aggregated loss reserve. Hence, capturing the dependence structure is vital for setting appropriate aggregated reserves. There are several interesting studies that address this issue, among others, Shi & Frees (2010)[2] and De Jong (2011)[3], who both use a parametric framework involving a copula approach.

1.2 Aim of the Thesis

This thesis focuses on the reserves for IBNR claims using run-off triangles. Its aim is to estimate the aggregated reserve for IBNR claims that is necessary for an insurer or reinsurer according to the regulatory requirements set by the Solvency regulations. In order to do this, IBNR from each LoB is separately modeled as a non-stationary marginal distribution, and the aggregated reserve is estimated using copulas to model the joint distribution. The purpose of this is to provide further information of the dependence structure in order to set more accurate aggregated reserves. Unlike the non-stationary marginal distributions used by Shi & Frees (2010), this method allows for non-positive values in the run-off triangle using the families in the Generalized Extreme Value distribution setting.

In order to benchmark the results, findings of the model are compared to the classical Chain Ladder methodology, where a bootstrap method has been applied. Additionally, the impact of dependence between LoBs is evaluated by comparing the results from the t-copula and Gaussian copula using the dependencies obtained, with the independent Gaussian copula, thus assuming independence between LoBs.

1.3 Limitations

When mentioning insurance, this thesis solely refers to non-life insurance. The properties of life insurance differ significantly from non-life insurance, and is outside the scope of the thesis.

Calendar year dependence within a run-off triangle is not something that will be taken into consideration in this thesis. Recent work which also involves non-stationary marginal distributions is from Abdallah, Boucher

and Cossette (2014)[4]. They incorporate calendar year dependence using a hierarchical Archimedean copula setting, such that the joint distributions between calendar years are used as input for the joint distribution between LoBs. This could be subject to further studies. Other previous work that incorporates calendar year effects in run-off triangles using a copula framework is de Jong (2010), who uses a model based on normal distributions.

1.4 Outline

The structure of the thesis is such that an introduction of the Solvency regulations is described in Chapter 2. The run-off triangle and the modeling thereof is presented in Chapter 3. In Chapter 4 the relevant theory behind copulas is defined. In Chapter 5 descriptions of validation methods are presented, in order to understand the implementation section in Chapter 6. Following the implementation, results are presented in Chapter 7 and conclusions and comments on the results are discussed in Chapter 8.

Chapter 2

2 Regulation

To assure that the policyholders are protected and to ensure stability in the financial market the insurance industry is restricted by regulations. The solvency margin is the regulatory required capital an insurance or reinsurance company is obliged to hold to cover for unforeseen events.

2.1 History

The available solvency margin was first defined in 1952, by T Pentikäinen, as the difference between assets and liabilities.[5] Though there were several methods for working out the solvency margin, the first formal set of non-life insurance regulations came in 1973. In these early days solvency assessments were based on simple formulas that were applied on accounting results. To calculate the required solvency margin one had to consider a sum of two results. The first was represented by investment risk and the second by technical risk, which refers to the risk of using the wrong claim rates. The models were simple to apply and easy to administer and understand, but they lacked the capability of covering for the increase in market complexity.

The drawbacks of these solvency requirements were examined in a report published in 1997 at a conference of insurance supervisory services in the European Union. As a result of this report, additional parameters were added. The development laid the foundation for modern insurance regulations, resulting in the introduction of Solvency I in the European Union in 2002.[6]

The idea behind Solvency I, as a EU-wide legalization, was to develop a single market of insurance services. Solvency I improved previous regulations with a robust method to regulate solvency of insurance companies but at

the same time it maintained its simplicity.

Some of the significant differences following the introduction of Solvency I was that the solvency requirements should be met at all times, not just at the time of the latest balance sheet. Another addition was that member states were given permission to set tighter regulations than those specified in the directives.[7]

2.2 Solvency II

Solvency I was primarily focused on capital adequacy for insurers but lacked inclusion of risk management and governance within firms. Hence, the introduction of an improved set of regulations was needed.

Solvency II is the latest solvency regulation which is, after several push-backs, scheduled to come into effect January 1, 2016.[8] The regulation is a risk-sensitive system for measuring the financial stability of insurance companies.

Solvency II is basically the insurance industry's counterpart to the Basel regulation of the banking industry. The architecture of Solvency II is, similarly to Basel's, built on a three pillar framework.

i. Pillar I - Capital adequacy, consists of resource requirements for the insurer to be considered solvent, ensuring policy holder protection.

ii. Pillar II - Systems of governance, sets requirements for the risk management and governance of the insurer.

iii. Pillar III - Supervisory reporting and public disclosure, ensuring greater transparency.[9]

For quantitative risk management purposes, there are two risk measures that are frequently being used. These risk measures are Value-at-Risk (VaR) and Tail Value-at-Risk (TVaR). The two are more specifically described below.

2.2.1 Value-at-Risk

Value-at-Risk is a measure to assess the risk associated with a portfolio of assets and liabilities. It is a quantile of the loss distribution and its definition

is presented below.

Definition 2.1: *Given some confidence level $\alpha \in (0,1)$, the VaR at a portfolio is given by the smallest number l such that the probability that a loss L exceeds l is no larger than (1-α).*

$$VaR_\alpha = \inf\{l \in \mathbb{R} : P(L > l) \leq 1 - \alpha\} \tag{2.1}$$

Solvency II requires that the insurer has enough capital to cover losses over the next twelve months with a probability of 99.5 percent, i.e. $VaR_{99.5\%}$.[10]

One of the drawbacks and main criticism with VaR is that it does not say anything about the severity of the loss in case the α-quantile is exceeded, as it does not consider the dynamics of the tail. Another critique concerns the subadditivity of VaR. Mathematically speaking, VaR is not a coherent risk measure[1] as the subadditivity condition does not always hold. If considering two losses L_1, L_2, the subadditivity is defined as

$$\varrho(L_1 + L_2) \leq \varrho(L_1) + \varrho(L_2) \tag{2.2}$$

where ϱ is a given risk measure.[11] Due to diversification benefits, this property is often considered a logical one within the risk management field, and is an incentive for copula theory within quantitative risk management on aggregated basis. As it does not always hold for VaR, the method may in some cases lead to nonsensical results.

2.2.2 Tail Value-at-Risk

Tail Value-at-Risk provides information about the average losses exceeding the α-quantile. In this way $TVaR_\alpha \geq VaR_\alpha$. Unlike VaR, TVaR also takes into account the tail properties of the distribution, as all α-exceedances are considered. This, in combination with TVaR being a coherent risk measure, makes it an attractive risk measure. TVaR is defined in Definition 2.2.

[1] For more information on coherent risk measures, see [11]

Definition 2.2 *The Tail Value-at-Risk of a portfolio is given by*

$$TVaR_\alpha = \frac{1}{1-\alpha}\int_\alpha^1 VaR_\alpha d\alpha \tag{2.3}$$

for a given confidence level $\alpha \in (0,1)$.[12]

There are several methods within Solvency II which are accepted standards for VaR and TVaR calculations. The technical specifications of Solvency II state that traditional actuarial techniques, for non-life insurance loss reserving, include estimations through run-off triangles. Apart from being a traditional tool within actuarial insurance, the run-off triangle methodology is now also an accepted method for regulatory purposes.[13]

Chapter 3

3 The Run-Off Triangle

3.1 Incurred But Not Reported Claims

It is not unusual that there is a time lag from the incident of an accident to the actual payment, these claims are called IBNR. There are several possible reasons for this, one is because of a delay in the reporting of an occurrence by the policyholder. Another reason is that it can take time to establish the actual cost of the claim. Property insurance is an example of this, it can take time to establish the consequences of an incident and payments can be made several years after the expiration of the contract. More strictly, IBNR claims refer to the difference between ultimate claims, i.e. matured or closed claims, and incurred claims. It consists of two parts

i. Pure IBNR - The reserves related to incurred events that have not yet been reported.

ii. Known claim reserves - The reserves for claims that have been reported but may have additional development.

3.2 Structure

When estimating IBNR, practitioners often assume a starting framework known as the run-off triangle. The run-off triangle is illustrated in Table 3.1. Its simplicity makes it easy to understand and provides an overview of the historical development of payments.

The run-off triangle is divided into cells where each cell corresponds to payments arising from a specific accident year $i \in \{1, \ldots, I\}$ and a development year $j \in \{0, \ldots, J\}$, where typically $I = J + 1$.

Table 3.1 The Run-off triangle

	Development Lag			
Accident Year	0	1	$\cdots$	J
1	$X_{1,0}$		$\cdots$	$X_{1,J}$
2		$\ddots$	$\iddots$	
$\vdots$	$\vdots$	$X_{i,j}$		
I	$X_{I,0}$	$\iddots$		

The accident year corresponds to the losses occurring during a given twelve-month period, and all premium earned during that same period, whereas the development year is typically the number of years after the incurred accident when a payment is made. Accident year is sometimes replaced by underwriting year, which is defined as all losses and premiums attributable to contracts signed or renewed within a given twelve-month period.[14] The calendar year k appears diagonally and is defined as $k = i + j$, with $k \leq I$, i.e. $k \in \{1, \ldots, I\}$. Then $X_{i,j}$ is defined as all incremental payments in accident year i with development j, where $i + j \leq I$, as $i + j > I$ has not yet occurred. In some settings cumulative payments $C_{i,j}$ are preferred such that $C_{i,n} = \sum_{j=1}^{n} X_{ij}$, with $C_{i,0} = X_{i,0}$. A general assumption regarding run-off triangles, which is basic for its application, is that claims have a lifetime of J years. After J years all claims are considered ultimate, i.e. claims are closed, such that $X_{i,j>J} = 0$.

One initially unintuitive aspect of the run-off triangle is the existence of negative values. As payments are defined as positive, negative values may result from non-premium cash inflows such as salvage recoveries, payments from third parties, internal errors, cancellation of outstanding claims due to initial overestimation of the loss or due to legal trials resulting in favor of the insurer.[15]

The main purpose of the run-off triangle is to attribute appropriate IBNR for the corresponding accident years. This corresponds to estimating the

future values below the triangle diagonal, which eventually forms a matrix. As is logical, claims that have not yet developed for long typically have higher IBNR than older claims. Hence, the lower part of the triangle, i.e. more recent and not far developed claims, generally have higher IBNR and are therefore of greater interest.

When inspecting the run-off triangle, large settlement amounts need to be investigated to find the cause of their size. Outliers that follow from single claims may undermine any method applied[2]. Therefore, adjustments of the data may be necessary in order to ensure realistic estimates.[13]

3.3 Interdependence

Within a run-off triangle certain dependencies arise for various reasons. Specifically there are three dependence patterns.

Horisontal Dependence Between specific accident years trends arise due to the time development from the incurred accident. This refers to the time development of payments, i.e. the horisontal trend in a run-off triangle. The logical explanation behind this is the nature of payments where payments typically decrease gradually with respect to time from the incurred accident, i.e. with respect to j. The development of payments differ depending on the contract and the LoB but the trend towards zero should be apparent in a normal setting.

Vertical Dependence Dependencies between development years will appear as a vertical trend in a run-off triangle. For an insurer or reinsurer, profitability in terms of sizes and amount of contracts signed will vary depending on several factors, such as macroeconomic effects, as well as industry and company specific factors. For instance, one can observe a cyclical pattern within the insurance industry known as the underwriting cycle. The cycle initially starts with a decrease in supply, raising premiums and un-

[2]The largest claims, such as catastrophe events and natural disasters, are generally handled separately due to their large impact.

derwriting standards[3] after a period of capital losses. The raised premiums and standards lead to a surge in profits, making the industry more attractive and therefore attracting competition. The increased competitiveness pushes margins downwards and relaxes standards, thereby completing the circle. The underwriting cycle can create a seasonal trend vertically.[16]

Looking at a broader perspective natural disasters are seeing increasing trend in both severity and frequency due to climate change, inducing an increasing trend for claims with natural disaster exposure. As an example, natural disasters between 2000 and 2009 were three times as many as between 1980 and 1989, with climate-related effects accounting for the majority of the increasing frequency.[17]

Calendar Year Dependence Calendar year effects appear diagonally in a run-off triangle, as these payments have occurred during the same calendar year. Thus, calendar year effects can arise due to macroeconomic effects such as inflationary trends and regulatory effects. One might also consider management related effects, such as a strategic push towards closing claims during a certain calendar year.

3.4 Cross Dependence

Typically run-off triangles are categorized by LoB. Hence, cross dependence refers to the dependence between triangles. Naturally, larger incidents such as natural disasters might have effects on several LoBs simultaneously. This dependence will have to be taken into account when modeling reserves on an aggregated entity level. Due to the interdependence in run-off triangles, capturing the actual cross dependence is cumbersome. As most run-off triangles exhibit a similar development year trend and are exposed to effects such as inflationary trends, this will create an overestimation of cross correlation if the interdependence is not extracted properly.

[3] Underwriting standard refers to the quality of cedents.

3.5 Modeling

3.5.1 Non parametric

3.5.1.1 Chain Ladder The Chain Ladder method is based on the assumption that the development pattern of claims observed in the past will continue in the future.

To find the development patterns between the development years one initially assumes a cumulative run-off triangle. The Chain Ladder method quantifies the development pattern using development factors defined as the average ratio between two consecutive development years. Mathematically, the development factors are calculated as

$$\hat{f}_j = \sum_{i=1}^{I-j} C_{i,j} / \sum_{i=1}^{I-j} C_{i,j-1}, \quad j \in \{1, \ldots, J\} \tag{3.1}$$

where $\hat{f}_j$ is the estimate for the development factors. Here, accident years $C_{i,1}, \ldots, C_{i,J}$, $i \in \{1, \ldots, I\}$ are assumed to be independent.

The development factors are then used to predict the future cumulative claims, i.e. the bottom right half of the triangle. This is done by multiplying the values found in the diagonal using $\hat{f}_j$ such that

$$\hat{C}_{i,j} = C_{i,I-i} \prod_{k=I+1-i}^{j} \hat{f}_k, \quad i + j \geq J + 2 \tag{3.2}$$

where $\hat{C}_{i,j}$ is the estimated future cumulative claim. This is illustrated in Table 3.2, where the observed values $C_{i,j}$ are found in the upper left half and the estimated values $\hat{C}_{i,j}$ in the bottom right respectively.

Table 3.2 Estimated Future Cumulative Claims

	Development Lag				
Accident Year	0	1	$\cdots$	$J-1$	J
1	$C_{1,0}$	$C_{1,1}$	$\cdots$	$C_{1,J-1}$	$C_{1,J}$
2				$C_{2,J-1}$	$\hat{C}_{2,J}$
		$\ddots$			
$\vdots$	$\vdots$		$\iddots$		
			$C_{i,j}$		$\vdots$
		$\iddots$	$\ddots$		
$I-1$	$C_{I-1,0}$	$C_{I-1,1}$			
I	$C_{I,0}$	$\hat{C}_{I,1}$	$\cdots$		$\hat{C}_{I,J}$

Once future estimates are calculated, the development factors $\hat{f}_j$ are used to obtain a back-fitted triangle, where the original claims $C_{i,j}$ are replaced by the predictive claims using (3.3). Back-fitting is done by dividing the values in the diagonal with $\hat{f}_j$ such that

$$\tilde{C}_{i,j} = \frac{C_{i,I-i}}{\prod_{k=j+1}^{I-i} \hat{f}_k}, \quad i+j \leq J \tag{3.3}$$

where $\tilde{C}_{i,j}$ is the back-fitted claim. The resulting back-fitted triangle is illustrated in Table 3.3.

Table 3.3 Back-fitted Triangle

	Development Lag				
Accident Year	0	1	$\cdots$	$J-1$	J
1	$\tilde{C}_{1,0}$		$\cdots$	$\tilde{C}_{1,J-1}$	$C_{1,J}$
2				$C_{2,J-1}$	
		$\ddots$			
$\vdots$	$\vdots$		$\iddots$		
			$C_{i,j}$		
		$\iddots$			
$I-1$	$\tilde{C}_{I-1,0}$	$C_{I-1,1}$			
I	$C_{I,0}$				

The next step is to calculate the residuals. For this calculation, one needs to define $C_{i,-1} = \tilde{C}_{i,-1} \equiv 0$. The residuals $r_{i,j}$ are then calculated as follows

$$r_{i,j} = \frac{(C_{i,j} - C_{i,j-1}) - (\tilde{C}_{i,j} - \tilde{C}_{i,j-1})}{\sqrt{\tilde{C}_{i,j} - \tilde{C}_{i,j-1}}}, \quad i + j \leq J + 1 \tag{3.4}$$

It is clearly seen from (3.4), for the equation to hold it requires $\tilde{C}_{i,j} - \tilde{C}_{i,j-1} > 0$, which in turn from (3.2) requires $\hat{f}_j > 1, \ \forall j$. This is a clear limiting factor for the Chain Ladder method and has been discussed in various actuarial theory.[15] Assuming this holds, a resulting residual triangle is obtained.

Table 3.4 Residual Triangle

	Development Lag				
Accident Year	0	1	$\cdots$	$J-1$	J
1	$r_{1,0}$		$\cdots$	$r_{1,J-1}$	$r_{1,J}$
2				$r_{2,J-1}$	
		$\ddots$			
$\vdots$	$\vdots$		$\iddots$		
			$r_{i,j}$		
		$\iddots$			
$I-1$	$r_{I-1,0}$	$r_{I-1,1}$			
I	$r_{I,1}$				

From the residual triangle, a bootstrap method[4] can be applied to calculate the reserves for each LoB.[18]

3.5.2 Parametric

For parametric models one is concerned with the modeling of incremental claims $X_{i,j}$ rather than the use of cumulative claims $C_{i,j}$. First $X_{i,j}$ is specified by $X_{i,j}^{(n)}$, $n \in \{1, \ldots, N\}$, with n denoting an insurer's nth portfolio, i.e. LoB.

Clearly, payments arising from an accident year i are much related to the number and sizes of contracts that were signed for the specific accident year, thus not being properly comparable. When studying dependence between triangles, the payments should therefore be independent of volumes and sizes of contracts. In order to properly evaluate dependence between triangles, they should be constructed in such a way that payments are considered with respect to its exposure. The precise quantity of exposure cannot be observed, therefore practitioners have used different measures to try to cap-

[4]The bootstrap simulation is found in appendix A.1.

ture the exposure appropriately.[19] The general setting is that the claims are exposure weighted such that $Y_{i,j}^{(n)} = X_{i,j}^{(n)}/\omega_i^{(n)}$, where $\omega_i^{(n)}$ is the exposure weight for triangle n in accident year i. Two general exposure weights exist where

i. $\omega_i^{(n)}$ equals the size of the premiums collected from accident year i.

ii. $\omega_i^{(n)}$ equals the amount of contracts signed during accident year i.

Both methods account for the exposure in their own way. However, the former does not take into account the premium variability from underwriting cycle effects, whereas the latter does not take into account the varying sizes of the contracts.

Due to triangle interdependencies, the applied marginal distribution needs to adapt to these dependencies. Before proceeding, the reader should take note as to how notations are being used in this thesis. As previously stated, variables in subscript denotes a particular index, whereas variables in parantheses imply a dependent variable. As such, the parametric marginal distribution is defined in the following manner

$$F^{(n)}(y_{i,j}^{(n)}; i, j) = P[Y^{(n)}(i, j) \leq y_{i,j}^{(n)}] = F^{(n)}(y_{i,j}^{(n)}; \eta^{(n)}(i, j), \zeta^{(n)}) \tag{3.5}$$

In the above equation, $F^{(n)}$ is the CDF from a marginal distribution. The $\eta^{(n)}(i, j)$ component denotes distribution parameters in $F^{(n)}(i, j)$, which are dependent on i and/or j, and $\zeta^{(n)}$ are other constant parameters in $F^{(n)}(i, j)$, independent of i and j.

Hence, the $\eta^{(n)}(i, j)$ component explains the distribution parameter(s) in terms of a function of explanatory variables that allows parameter(s) to vary with respect to i and/or j, thus adapting to the properties of the data. One could typically consider each parameter in $\eta^{(n)}(i, j)$ as a regression model to fit the data. As such, $\eta(i, j)$ can be expressed in a general setting as

$$\eta^{(n)}(i, j) = \varphi^{(n)} + \alpha^{(n)}(i) + \beta^{(n)}(j) + \delta^{(n)}(i + j) \tag{3.6}$$

with the respective parameters depending on each triangular interdepen-

dence respectively[5]. Here, the initial varying parameters start from zero, i.e. $\alpha^{(n)}(1) = 0$, $\beta^{(n)}(0) = 0$ and $\delta^{(n)}(1) = 0$. In cases where $\eta^{(n)}(i,j)$ consists of more than one distribution parameter, the above equation assumes a vector form

$$\bar{\eta}^{(n)}(i,j) = \bar{\varphi}^{(n)} + \bar{\alpha}^{(n)}(i) + \bar{\beta}^{(n)}(j) + \bar{\delta}^{(n)}(i+j) \tag{3.7}$$

In order to check the validation of the fitted distribution using one-sample goodness of fit measures, one will need to transform the data in order to make it independent of any trend parameters $\eta^{(n)}(i,j)$, as the random variables for the respective margins are required to be iid.

The parametric distributions commonly used in the field of modeling incremental run-off triangles are log-normal and gamma distributions. Since these require the assumption of positive incremental claims, other methods which relax this assumption have been studied. Alba & Corzo (2005)[15] have addressed the issue by introducing a three parameter log-normal model that is able to account for negative values.

3.5.2.1 Generalized Extreme Value Distribution The generalized extreme value distribution (GEV) is regarded as one of the cornerstones in extreme value theory. It is often applied when modeling block maxima, i.e. maxima for given intervals from a set of observations. For instance, given observations $X_1, \ldots, X_N$, one might be interested in the behavior of maxima $M_n = \max(X_1, \ldots, X_n)$ within sequences of length n, resulting in $M_{n,1}, \ldots, M_{n,N/n}$ maxima that are to be modeled.

Within the GEV distribution there are three families - Fréchet, Weibull and Gumbel. They all share a general distribution function of the form

$$GEV(x; \mu, \sigma, \gamma) = \exp\left\{ -\left(1 + \gamma \frac{x-\mu}{\sigma}\right)^{-1/\gamma} \right\}, \tag{3.8}$$

where $\mu \in \mathbb{R}$ is denoted as the location parameter, $\sigma > 0$ as the scale parameter and $\gamma \in \mathbb{R}$ as the shape parameter. What differentiates the three

[5]Note that δ is the calendar year dependence, as $k = i + j$.

families is the shape parameter. For Fréchet $\gamma > 0$, Weibull $\gamma < 0$, and for Gumbel $\gamma = 0$. Consequently, the families have different support with the following bounds[20]

$$\begin{aligned} Fréchet(\mu, \sigma, \gamma) &\in [\mu - \sigma/\gamma, \infty) \\ Weibull(\mu, \sigma, \gamma) &\in (-\infty, \mu - \sigma/\gamma] \\ Gumbel(\mu, \sigma) &\in (-\infty, \infty) \end{aligned} \tag{3.9}$$

For a clearer illustration, the density plots are shown in Figure 3.1. As can clearly be seen, the upper tail for the families without an upper bound is substantially larger than the standard normal distribution.

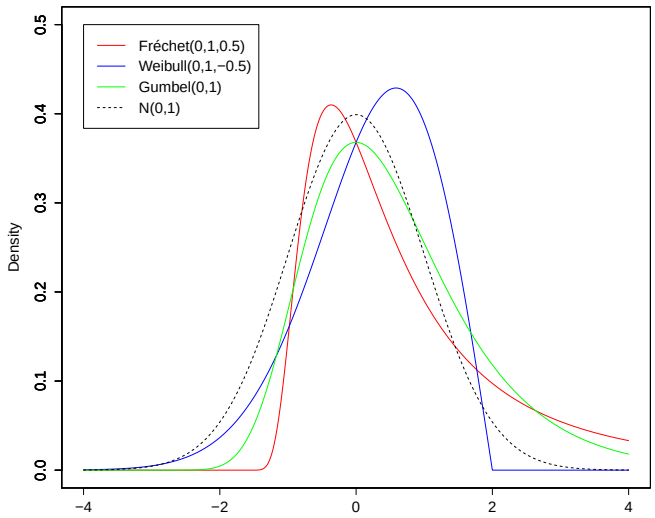

Figure 3.1: *Density plots of the GEV families compared to a standard normal distribution.*

Any GEV distribution can be transformed to the standard Gumbel distribution, i.e. $GEV(0, 1, 0)$ using Definition 3.1.[6]

Definition 3.1 *Let $X \sim GEV(\mu, \sigma, \gamma)$, with $\mu \in \mathbb{R}$, $\sigma > 0$ and $\gamma \in \mathbb{R}$. Then $\tilde{X}$ of the form*

[6] For the full derivation, see appendix A.2.

$$\tilde{X} = \frac{1}{\gamma} \ln \left(1 + \gamma \frac{X - \mu}{\sigma} \right) \tag{3.10}$$

is standard Gumbel distributed.

3.5.2.2 Parameter Estimation

Maximum Likelihood Estimation Maximum likelihood estimation (MLE) is a flexible method for estimation of the unknown distribution parameters $\theta = (\theta_1, \ldots, \theta_n)$. Its principle is based on maximizing the probability that a given data set belongs to a distribution F_θ, using the parameters θ. Suppose that $\mathbf{X} = (X_1, \ldots, X_n)$ are independent realizations of a parametric family $f_X(x, \theta)$. The likelihood function for the parameter θ is given by

$$\mathcal{L}(\theta; \mathbf{X}) = \prod_{i=1}^{n} f(X_i; \theta) \tag{3.11}$$

It is often more practical to work with the logarithms of the likelihood values instead. The log-likelihood function is defined as

$$\ln \mathcal{L}(\theta; \mathbf{X}) = \sum_{i=1}^{n} \ln f(X_i; \theta) \tag{3.12}$$

The optimal values $\hat{\theta}_{MLE}$ are defined as the values of θ that maximize the likelihood function

$$\hat{\theta}_{MLE} = \arg \max_{\theta} \ln \mathcal{L}(\theta; \mathbf{X}) \tag{3.13}$$

The obtained distribution $f(\mathbf{X}, \hat{\theta}_{MLE})$ is then considered the distribution that best describes the observed data $\mathbf{X}$.[20]

Looking at an aggregated level, the obtained marginal distributions provide as input in the modeling of the joint distribution. If considering parametric models for run-off triangles it is natural to apply copula theory for aggregated loss reserving. Hence, one is able to use the entire collection of copulas and its respective properties for estimation, stress testing and regulatory reporting purposes.

Chapter 4

4 Copulas

The usage of copula has during the last two decades gained popularity in the fields of applied mathematics, especially in finance, insurance and reliability theory. As regulations have tightened in the insurance and finance industry, following the Solvency and Basel frameworks, incentives for the usage of copulas have increased. The incentives come from the ability to express dependence on a quantile scale and thereby obtain risk measures required by the regulations, and more importantly, to improve risk management activities in general.[21]

Assume that $X_1, \ldots, X_n$ are random variables with distribution functions $F_1(x_1) = P[X_1 \leq x_1], \ldots, F_n(x_n) = P[X_n \leq x_n]$, respectively, and a joint distribution function $H(x_1, \ldots, x_n) = P[X_1 \leq x_1, \ldots, X_n \leq x_n]$. The joint distribution function of the random variables contains both a description of the marginal behavior of the individual variables as well as information about the dependency structure between them. Copulas allow for a bottom-up approach, separating the marginal distribution from the dependence structure and modeling these separately. The flexibility of choosing marginal distributions free of choice and the extensive collection of copulas with various properties give the ability to model joint distributions at a deeper level. Additionally, copulas are easily simulated, thus being useful in Monte Carlo simulations.

The essentials of copulas in studying the multivariate distribution functions are summarized in the following theorem.

Theorem 4.1 (Sklar's theorem)

Let H be a joint distribution function with margins $F_1, \ldots, F_n$. Then there exists a copula which is mapping the unit hypercube into the unit interval, $C : [0,1]^n \to [0,1]$, such that for all $x_1, \ldots, x_n \in \mathbb{R}$

$$H(x_1, \ldots, x_n) = C(F_1(x_1), F_2(x_2), \ldots, F_n(x_n)) \tag{4.1}$$

If the margins are continuous, then C is unique; otherwise, C is uniquely determined on $\operatorname{Ran} F_1 \times \operatorname{Ran} F_2 \times \ldots \times \operatorname{Ran} F_n$ *where* $\operatorname{Ran} F_i = F_i(\mathbb{R})$ *denotes the range of F_i. Conversely, if C is a copula and $F_1, \ldots, F_n$ are univariate distribution functions, then the function H defined by* (4.1) *is a joint distribution function with margins $F_1, \ldots, F_n$.*[11]

Corollary 4.1

Let H, C, $F_1, \ldots, F_n$ be defined as in Theorem 4.1*, and define $u_1, \ldots, u_n = F_1(x_1), \ldots, F_n(x_n)$. Further, let $F_1^{(-1)}, \ldots, F_n^{(-1)}$ be the quasi-inverses of $F_1, \ldots, F_n$, respectively. Then the following holds*

$$C(u_1, \ldots, u_n) = H(F_1^{(-1)}(u_1), \ldots, F_n^{(-1)}(u_n)) \tag{4.2}$$

for any $\mathbf{u}$ *in* $[0,1]^n$[22]

For C to be a copula, the following three properties most hold.

i. $C(u_1, \ldots, u_n)$ is increasing in each component of u_i.

ii. $C(1, \ldots, 1, u_i, 1, \ldots, 1) = u_i$ for all $i \in \{1, \ldots, n\}$, $u_i \in [0,1]$.

iii. For all $(a_1, \ldots, a_n), (b_1, \ldots, b_n) \in [0,1]^n$ with $a_i \leq b_i$ we have

$$\sum_{i_1=1}^{2} \ldots \sum_{i_n=1}^{2} (-1)^{i_1 + \ldots + i_n} C(u_{1i_1}, \ldots, u_{ni_n}) \geq 0 \tag{4.3}$$

where $u_{j1} = a_j$ and $u_{j2} = b_j$ for all $j \in \{1, \ldots, n\}$[11]

4.1 Dependence measures

4.1.1 Linear Correlation

Pearson's rho, ρ_P One of the most frequently used correlation measures is Pearson's linear correlation. It is, in the bivariate case, defined by

$$\rho_P(\mathbf{X}, \mathbf{Y}) = \frac{\text{cov}(\mathbf{X},\mathbf{Y})}{\sqrt{\text{var}(\mathbf{X})\text{var}(\mathbf{Y})}} = \frac{\mathbb{E}[(\mathbf{X}\text{-}\mu_{\text{X}})(\mathbf{Y}\text{-}\mu_{\text{Y}})]}{\sqrt{\text{var}(\mathbf{X})\text{var}(\mathbf{Y})}} \tag{4.4}$$

In the copula framework, Pearson's correlation depends on the copula of a bivariate distribution as well as the marginal distributions. An obvious weakness with Pearson's correlation is that it only measures linear dependence. Furthermore, it is only invariant in the case of strictly increasing linear transformations and not in the case of nonlinear strictly increasing transformations.

4.1.2 Rank Correlation

Rank correlations are measures of dependence which, unlike Pearson's correlation, only depend on the copula of a bivariate distribution and not the marginal distributions. The standard empirical estimator of rank correlation is calculated by looking at the ordering of the sample for each variable instead of the numerical values, also known as concordance.

Definition 4.1 *Two observations in $\mathbb{R}^2$, (x_i, y_i) and (x_j, y_j), are denoted as concordant if $(x_i - x_j)(y_i - y_j) > 0$, and discordant if $(x_i - x_j)(y_i - y_j) < 0$.*[11]

Kendall's tau, τ_K Let $\{(x_1, y_1), \dots (x_n, y_n)\}$ denote a random sample of n observations from vectors $(\mathbf{X}, \mathbf{Y})$ of continuous random variables. There are $\binom{n}{2}$ distinct pairs (x_i, y_i) and (x_j, y_j) of observations in the sample. Let c denote the number of concordant pairs and d denote the number of discordant pairs. Then Kendall's tau for the sample is defined as

$$\tau_K(\mathbf{X}, \mathbf{Y}) = \frac{c-d}{c+d} = \frac{(c-d)}{\binom{n}{2}} \tag{4.5}$$

This is equivalent with τ_K being equal to the probability of concordance minus the probability of discordance for a pair of observations (x_i, y_i) and (x_j, y_j) that are chosen randomly from the sample.

Let $(\mathbf{X}_1, \mathbf{Y}_1)$ and $(\mathbf{X}_2, \mathbf{Y}_2)$ be iid random vectors, then the population version of Kendall's tau is defined as

$$\tau_K(\mathbf{X}, \mathbf{Y}) = \mathbb{P}[(\mathbf{X}_1 - \mathbf{X}_2)(\mathbf{Y}_1 - \mathbf{Y}_2) > 0] - \mathbb{P}[(\mathbf{X}_1 - \mathbf{X}_2)(\mathbf{Y}_1 - \mathbf{Y}_2)] < 0] \tag{4.6}$$

Relating to copula theory, assume that X and Y have the copula C, Kendall's tau is then defined as

$$\tau_K(\mathbf{X}, \mathbf{Y}) = 4 \iint_{[0,1]^2} C(u, v) dC(u, v) - 1 = 4\mathbb{E}[C(u, v)] - 1 \tag{4.7}$$

4.1.3 Tail dependence

Tail dependence describes the dependence between the variables in the upper right quadrant as well as in the lower left quadrant of the unit square $[0, 1]^2$.

Definition 4.2 *Let X and Y be continuous random variables with distribution functions F and G, respectively. The coefficient of upper tail dependence, λ_u, is the limit of the conditional probability that Y is greater than the $100t$-th percentile of G given that X is greater than the $100t$-th percentile of F as t approaches 1, i.e.*

$$\lambda_u = \lim_{t \to 1^-} P[Y > G^{(-1)}(t) | X > F^{(-1)}(t)] \tag{4.8}$$

provided a limit $\lambda_u \in [0, 1]$ exists. If $\lambda_u \in (0, 1]$, X and Y are said to show upper tail dependence. If $\lambda_u = 0$, they are asymptotically independent in the upper tail.

Similarly, λ_l is the limit of the conditional probability that Y is less than or equal to the $100t$-th percentile. Concerning copula theory, the relation is described in Theorem 4.2 below.

Theorem 4.2 *Let X, Y, F, G and λ_u be defined as in Definition 4.2, and let C be the copula of X and Y, with diagonal section δ_C[7]. If the limits for λ_u exists as in (4.8), then*

$$\lambda_u = 2 - \lim_{t \to 1^-} \frac{1 - C(t,t)}{1-t} = 2 - \delta\,'_C(1^-) \tag{4.9}$$

Similarly, λ_l is defined as[22]

$$\lambda_l = \lim_{t \to 0^+} \frac{1 - C(t,t)}{t} = \delta\,'_C(0^+) \tag{4.10}$$

4.2 Elliptical Copulas

Elliptical copulas is a family of symmetrical copulas for which the dependence structure can be described by the correlation matrix Σ. Thus, elliptical copulas have the advantage of being able to apply different correlations between distributions for dimensions higher than the bivariate case.

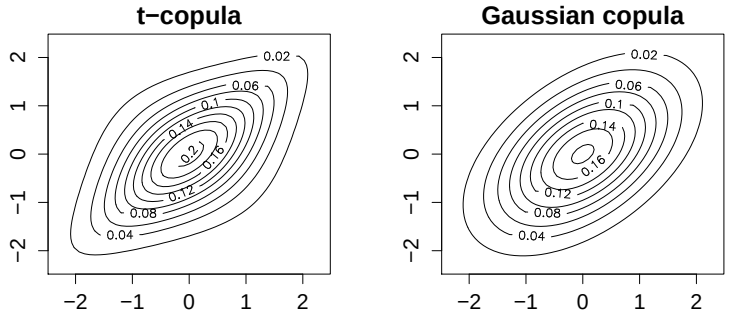

Figure 4.1: *Contour plots describing the density for the t-copula and Gaussian copula with $\rho = 0.5$.*

[7]The diagonal section δ_C is defined by $\delta_C(t) = C(t,t)$.

For all elliptical copulas, the relationship between its dependence parameter and Kendall's τ is of the form

$$\tau_K = \frac{2}{\pi} \arcsin \rho \tag{4.11}$$

Where ρ is the corresponding off-diagonal dependence parameter in Σ.

Gaussian copula Gaussian copula, also known as normal copula, is a representation of the multivariate normal distribution. Its distribution function is not available in closed form. However, its density function is, and it is structured as

$$c(\mathbf{u}) = \frac{1}{|\Sigma|^{1/2}} \exp\left\{-\frac{1}{2}\mathbf{u}^T\left(\Sigma^{-1} - I\right)\mathbf{u}\right\} \tag{4.12}$$

where $\mathbf{u} = (u_1, \ldots, u_n)$ and $\Sigma_{i,j} = \frac{cov(x_i,x_j)}{\sqrt{var(x_i)var(x_j)}}$, known as the correlation matrix.[23] Its relation to the normal distribution makes it intuitive and familiar, therefore it is often the copula of choice in many field of applications.

With regards to risk management, the normal copula has recently been criticized for not exhibiting any tail dependence. We have come to learn that increased levels of stress, for instance in financial markets, have a tendency of inducing additional dependence. As such, the normal copula would not be a suitable choice in this regard as it cannot capture this feature, therefore underestimating stressful scenarios.

***t*-copula** Similarly to the Gaussian copula, the t-copula is a representation of the multivariate t-distribution, where the density function is given by

$$c_\nu(\mathbf{u}) = \frac{\Gamma(\frac{\nu+n}{2})\Gamma(\frac{\nu}{2})^{n-1}(1 + \frac{\mathbf{x}'\Sigma^{-1}\mathbf{x}}{\nu})}{|\Sigma|^{1/2}} \tag{4.13}$$

here, ν is the degrees of freedom, n is the dimension, and Γ is the gamma function.

As can be seen in Figure 4.1, the t-copula has more outliers. Additionally, for risk management purposes it has the attractive property of exhibiting tail dependence, which can be observed in the upper and lower tail. The

tails are symmetric and its tail dependence is of the form

$$\lambda = 2t_{\nu+1}\left\{-\left[(\nu-1)\frac{1-\rho}{1+\rho}\right]^{1/2}\right\} \tag{4.14}$$

where ρ is the off diagonal element of Σ and $t_{\nu+1}$ is the t-distribution function.[24]

Chapter 5

5 Model Validation

5.1 Likelihood Ratio Test

The likelihood ratio test is limited to the comparison of nested models, i.e. one of the two models being compared has to form a special case of the other. Rather than giving information about the general fit of a model, the test is a way to select the most appropriate one.

To test if the null hypothesis $H_0 : \theta \in \Theta_0$ against the alternative hypothesis $H_1 : \theta \in \Theta$, where $\Theta_0 \subset \Theta$, one can perform the likelihood ratio test, defined as

$$\lambda(\mathbf{X}) = \frac{\sup_{\theta \in \Theta_0} \mathcal{L}(\theta; \mathbf{X})}{\sup_{\theta \in \Theta} \mathcal{L}(\theta; \mathbf{X})} \tag{5.1}$$

It can be shown that

$$-2 \ln \lambda(\mathbf{X}) \sim \chi^2_\upsilon \tag{5.2}$$

where the degrees of freedom parameter υ of the chi-squared distribution is given by the number of free parameters in Θ minus the ones specified in Θ_0.

The null hypothesis is rejected if $-2 \ln \lambda(\mathbf{X}) > q_{\upsilon,\alpha}$, where $q_{\upsilon,\alpha}$ is the α-quantile of the χ^2_υ distribution.[11]

5.2 Information Criteria

Information criteria are methods that deal with the comparison of non-nested models with possibly quite different number of parameters. Unlike the likelihood ratio test, these approaches penalize the models according to the number of parameters they use. As additional parameters never decrease the MLE value, this penalization accounts for parameter uncertainty in the model. The following two criterias use the notations described below.

Suppose there are m models $M_1, \ldots, M_m$ and that model l has k_l parameters denoted by $\theta_l = (\theta_{l1}, \ldots \theta_{lk_l})$ and a likelihood function $\mathcal{L}_l(\theta_l; \mathbf{X})$. Let $\hat{\theta}_l$ denote the maximum likelihood estimation of θ_l.

5.2.1 Akaike Information Criteria

According to Akaike's information criteria (AIC), the model closest to the true model is the one minimizing

$$AIC(M_l) = -2 \ln \mathcal{L}_l(\hat{\theta}_l; \mathbf{X}) + 2k_l \tag{5.3}$$

AIC is useful when selecting the best model in a set without saying anything about the quality of that model. If all the models in the set give poor results, AIC will still select the one that gives the best estimate, even though that estimate might be poor in an absolute sense.

5.2.2 Bayesian Information Criteria

According to the Bayesian information criteria (BIC), the most appropriate model is the one minimizing

$$BIC(M_l) = -2 \ln \mathcal{L}(\hat{\theta}_l; \mathbf{X}) + k_l \ln(n) \tag{5.4}$$

where n is the number of observations. For $ln(n) > 2$, BIC penalizes model complexity more than AIC. Given this, the only way they will give different results is when AIC chooses a more complex model than BIC.[25]

5.3 The Auto-Correlation Function

The auto-correlation function (ACF) is a convenient tool that identifies trends, seasonality and/or interdependencies in time-series data. It measures the correlation between y_t and y_{t-k}, where $k \in \mathbb{N}$ denotes the lag parameter. For instance, if considering two daily stock prices y_{t-k} and y_t, the lag parameter k denotes the number of days between the two daily closing prices. The ACF is frequently used in time series modeling, with

applications for risk management purposes. The ACF of y_t is defined as

$$\rho_y(k) = \frac{r_y(k)}{r_y(0)}, \qquad k \in \mathbb{N} \tag{5.5}$$

where r_y is the auto-covariance function for y_t defined as

$$r_y(k) \equiv C\{y_t, y_{t-k}\} \triangleq \mathbb{E}\left\{(y_t - \mathbb{E}[y_t])(y_{t-k} - \mathbb{E}[y_{t-k}])\right\} \tag{5.6}$$

$\rho_y(k)$ is bounded such that $|\rho_y(k)| \leq 1$, with $\rho_y(0) = 1$, as is general for any correlation measures. The time series is considered independent when $\rho_y(k) = 0$ for $k > 0$.[26]

5.4 Kolmogorov-Smirnov

Kolmogorov-Smirnov test is a goodness of fit test based on the empirical distribution of a random sample.

Let $(x_1, \ldots, x_n)$ be observations from iid random variables $(X_1, \ldots, X_n)$ with distribution function F. In the univariate case one can test the hypothesis, $H_0 : F = F_0$ against $H_1 : F \neq F_0$ where F_0 is some specified distribution function, using the Kolmogorov-Smirnov test.

The one-sample test describes the maximum distance between the empirical distribution function and its corresponding theoretical distribution function. The test is defined as

$$D_n = \sup_{x \in \mathbb{R}} |\hat{F}_n(x) - F(x)| \tag{5.7}$$

where $\hat{F}_n(x)$ is the empirical distribution function of the sample. The null hypothesis is rejected if $D_n > D_{crit}$, where the critical value is a function of the significance level as well as the number of samples.[27]

5.5 Cramér-von Mises

Cramér-von Mises can be used to test the goodness of fit for a copula. First one defines the empirical copula as

$$C_n(\mathbf{u}) = \frac{1}{n}\sum_{i=1}^{n} \mathbf{1}(\hat{U}_{i,1} \leq u_1, \ldots, \hat{U}_{i,d} \leq u_d),\ i \in \{1, \ldots, n\} \tag{5.8}$$

where $\mathbf{u} = (u_1, \ldots, u_d) \in [0,1]^d$. The goodness of fit test is then based on the empirical process

$$\mathbb{C}_n(\mathbf{u}) = \sqrt{n}(C_n - C_{\theta,n}) \tag{5.9}$$

where $C_{\theta,n}$ is an estimator of C obtained under the null-hypothesis H_0 : $C \in \mathcal{C}_0$ for some class $\mathcal{C}_0$ of copulas. θ_n is the estimate of θ derived from the pseudo-observations.

Based on the empirical process one can calculate the Cramér-von Mises statistic as[28]

$$S_n = \int_{[0,1]^d} \mathbb{C}_n(\mathbf{u})^2 dC_n(\mathbf{u}) \tag{5.10}$$

A large value of S_n leads to rejection of the null-hypothesis. The main inconvenience with this approach is its high computational cost[8].

[8]For further derivations of S_nC see Genest et al. (2009)[28]

Chapter 6

6 Implementation

The data used has been collected from Sirius International, a Swedish-based reinsurer with a globally diversified business portfolio. Three of its main LoBs, $n \in 1, 2, 3$, as defined in Section 3.5.2, are Aviation, Marine and Property respectively. Data includes the development interval 0 to 13.5 years dating back to 2001 ($I = 13$). As is standard practice, individual extreme losses have been extracted before data has been implemented in a run-off triangle framework, categorized by each LoB respectively. Because of the shortage of values in run-off triangles, development data has been provided on a quarterly basis ($J = 53$) in order to cope with problems arising from lack of data values as well as information lost from merging the data. Due to the decreasing relevance of data for longer matured claims and for optimization efficiency, the modeling is focused on claims with maturity up to 4.5 years, i.e. $J = 17$. Since the data is divided into accident years and development quarters, the run-off triangle will be asymmetrical. Despite the asymmetry and the fact that development has been limited to 4.5 years, previously stated run-off triangle methodology can be applied in this setting.

In this thesis, the exposure weight introduced is defined as $\omega_i^{(n)} = UltPr_i^{(n)} \cdot LR_i^{(n)}$ such that payments $X_{i,j}^{(n)}$ are exposure weighted of the form

$$Y_{i,j}^{(n)} = \frac{X_{i,j}^{(n)}}{UltPr_i^{(n)} \cdot LR_i^{(n)}} \tag{6.1}$$

Here, $UltPr_i$ is the estimated final (ultimate) premium revenue from contracts signed in accident year i. LR_i is the forward looking Loss ratio[9].

[9]The estimation of $UltPr_i$ and LR_i has been performed by Sirius International, and is taken as given in this thesis.

In this case, the loss ratio LR_i is set beforehand and is a projection of future profitability. In a sense, LR_i somewhat helps to offset varying market profitability effects, much related to the underwriting cycle, which for some LoBs can be substantial[10].

6.1 Data Assumptions

The data provided by Sirius International is on underwriting year rather than accident year basis. A difference between the two reporting measures will appear in cases where the accident occurs in a year different from the year underwriting was made. If reporting on underwriting year basis, payments are assigned to the year the contract was signed, i.e. underwriting year, independently of when the accident occurs.

As inception date has not been provided, contracts are assumed to be signed in the beginning of each year, such that payment development is with respect to January 1. This assumption is valid in most cases, but not all.[29] Therefore, the development lag might be overestimated in the cases when the inception date is not the beginning of the year.

One could consider modeling dependence between contract types. However, no regard is taken to the types of contracts as these are aggregated in order to obtain run-off triangles on LoB level. In reality, they have different properties and will therefore affect payments differently.

6.2 Data Analysis

The exposure weighted payments $Y_{i,j}^{(n)}$ are summarized in Table 6.1, and their development over time is displayed in Figure 6.1. The finer development granularity illustrates an initial increasing trend, which would not be captured appropriately by annual development data categorization. One can also see a tendency in which Marine affairs typically have a longer delay. The commonly shared pattern is a shifting average as well as a varying volatility depending on development quarter j.

[10] Aviation is an example of contracts that are sensitive to market conditions.

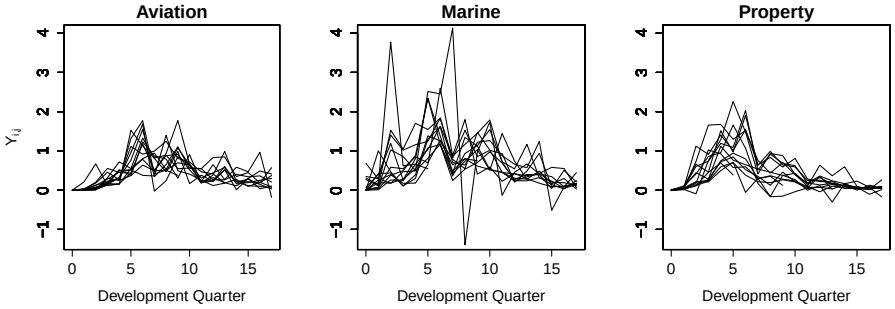

Figure 6.1: *Time series plots for exposure weighted data, where each line corresponds to a fixed underwriting year.*

Table 6.1 Summary Exposure Weighted Data

LoB	Mean	Min	Max	Standard Deviation
Aviation	0.4189	-0.1820	1.775	0.3802
Marine	0.6625	-1.390	4.128	0.6476
Property	0.3556	-0.3033	2.257	0.4530

As for non-positive values, an average of six percent is below or equal to zero, with 39 percent of them being negative. If one were to consider a longer development, the share of negative values would be likely to increase as they tend to occur more frequently at a later development stage[11]. Due to the non-positive data, it is clear that the commonly used gamma and log-normal distributions of its original form are not applicable.

In order to verify current dependencies, the ACF for $Y^{(n)}$ is examined across underwriting years, as well as development quarters. ACF plots for underwriting years and development years are provided in Figure 6.2 and Figure 6.3 respectively[12].

The accuracy of the ACF when validating vertical dependence is very low due to the limitation of data points, as $I = 13$. This is reflected in

[11]For the fully developed data, i.e. $J = 53$, the corresponding figures are 11 percent, with 76 percent being negative values.

[12]The ACF figures in this thesis only present one row and column for each LoB as examples. The actual verification needs to take all rows and columns into account.

the wide confidence interval provided in the figure. For higher development quarters, the accuracy decreases further as the number of data points is even less for higher columns. The lag parameter k has been limited to $k \leq 4$, since the data set looses k values in the validation of $\rho_Y(k)$. Nevertheless, given the overall view, there are no significant correlations and no apparent patterns between the autocorrelation functions. Thus, independence across underwriting years, i.e. vertical dependence, is assumed on the 95 percent confidence interval provided.

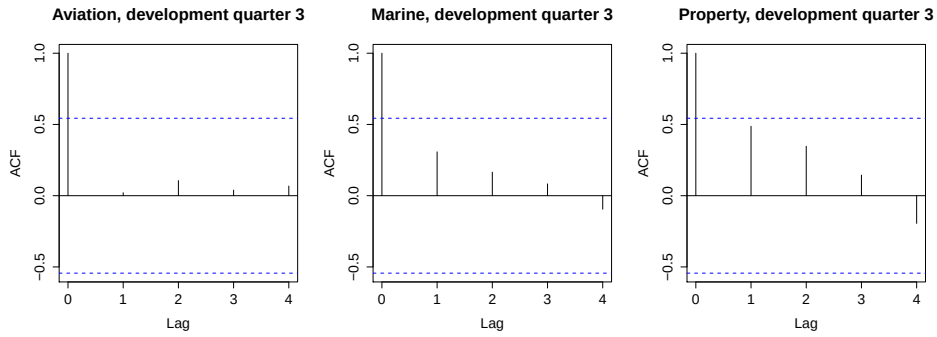

Figure 6.2: *ACF plots illustrating vertical dependence. The dashed blue lines represent a 95 percent confidence interval.*

As for horisontal dependence the trend that is seen in Figure 6.1 is confirmed by the repetitive pattern of the ACF in Figure 6.3. The initial increase followed by the downward trend in the data is reflected as a positive correlation for low k, and a negative correlation for larger k. Before modeling using copulas, this correlation will have to be extracted properly. Note the somewhat tighter confidence interval obtained thanks to a slight increase in number of data points $J + 1 = 18$.

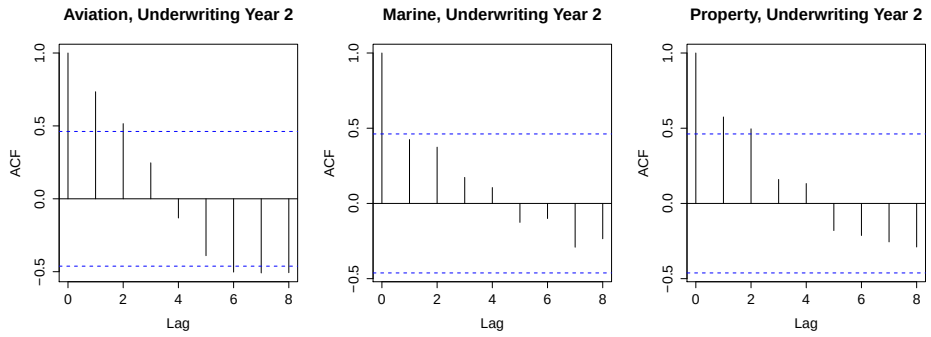

Figure 6.3: *ACF plots illustrating horisontal dependence. The dashed blue lines represent a 95 percent confidence interval.*

6.3 Non-Stationary Marginal Distributions

As stated earlier, one can see a parallel shift in the data, as well as a varying volatility with respect to development. Although GEV distributions are commonly applied for modeling of maxima, its properties and appearance makes it a reasonable choice in other applications. If one were to apply a GEV distribution to this data, one could consider an adaptive location and scale parameter to capture each dynamic respectively. Since it has been concluded that no vertical trend exists, the GEV distribution can be expressed as

$$Y^{(n)}(j) \sim GEV(\mu^{(n)}(j), \sigma^{(n)}(j), \gamma^{(n)}) \tag{6.2}$$

Referring back to (3.5), $\zeta^{(n)} = \gamma^{(n)}$, with the $\bar{\eta}^{(n)}(i,j)$ component defined as

$$\bar{\eta}^{(n)}(i,j) = \begin{pmatrix} \mu^{(n)}(j) \\ \sigma^{(n)}(j) \end{pmatrix} \tag{6.3}$$

As $\bar{\eta}^{(n)}(i,j)$ only depends on j, this implies that in (3.7), $\bar{\alpha}^{(n)}(i), \bar{\delta}^{(n)}(i+j) = 0$ for all i,j, and so $\bar{\eta}^{(n)}(i,j)$ is reduced to $\bar{\eta}^{(n)}(j)$. The implication of this is that each non-stationary distribution $Y^{(n)}(j)$ will consist of J stationary distributions.

In order to cope with the various trends of $\mu^{(n)}(j)$ and $\sigma^{(n)}(j)$, the following regression model is applied where increasing values of l and m are tested

$$\bar{\eta}^{(n)}(j) = \begin{pmatrix} \mu^{(n)}(j) \\ \sigma^{(n)}(j) \end{pmatrix} = \begin{pmatrix} \sum_{k=0}^{l} \mu_k^{(n)} j^k \\ \sum_{k=0}^{m} \sigma_k^{(n)} j^k \end{pmatrix} \tag{6.4}$$

Again, referring back to (3.7), the above equation corresponds to

$$\bar{\varphi}^{(n)} = \begin{pmatrix} \mu_0 \\ \sigma_0 \end{pmatrix}, \; with \; \bar{\beta}^{(n)}(j) = \begin{pmatrix} \sum_{k=1}^{l} \mu_k^{(n)} j^k \\ \sum_{k=1}^{m} \sigma_k^{(n)} j^k \end{pmatrix} \tag{6.5}$$

Thus, $Y^{(n)}(j)$ will henceforth be denoted $Y_{l,m}^{(n)}(j)$, where parameters $\mu^{(n)}(j)$, $\sigma^{(n)}(j)$ and $\gamma^{(n)}$ are to be estimated for each LoB n respectively. The validation of $Y_{l,m}^{(n)}(j)$ is done using the following process

i. Obtaining MLE parameters $\hat{\theta}_{MLE}^{(n)} = (\mu^{(n)}(j), \sigma^{(n)}(j), \gamma^{(n)})$ for each $Y_{l.m}^{(n)}(j)$, where log-likelihood values are obtained. Since $\sigma^{(n)}(j) > 0, \forall\, j$ is required, the MLE is performed using the constrained linear optimization constrOptim, implemented in R. For any linear trend in $\sigma^{(n)}(j)$, constrOptim will be sufficient. When non-linearity in $\sigma^{(n)}(j)$ holds, a simple penalized MLE is introduced such that the value 100 is subtracted for every term in $\ln \mathcal{L}(\bar{\eta}^{(n)}(j), \gamma^{(n)} : \mathbf{Y}(j))$ where $\sigma^{(n)}(j) < 0$.

ii. The obtained models $Y_{l,m}^{(n)}(j)$ from MLE are compared using the three validation methods stated in Chapter 5 - Likelihood ratio test, AIC and BIC.

iii. In order to verify the performance of the estimated parameters, Definition 3.1 is applied such that, if parameter estimation is true, the transformed data $\tilde{Y}^{(n)} \sim Gumbel(0, 1)$. Since $Y^{(n)}$ is non-stationary, i.e. not identically distributed, Definition 3.1 adopts to

$$\tilde{Y}^{(n)} = \frac{1}{\gamma^{(n)}} \ln \left(1 + \gamma^{(n)} \frac{Y_j^{(n)} - \mu^{(n)}(j)}{\sigma^{(n)}(j)} \right) \tag{6.6}$$

Following the transformation, a one-sample Kolmogorov-Smirnov goodness of fit is conducted against the theoretical standard Gumbel. Furthermore, visual comparisons between the obtained empirical distribution and the theoretical standard Gumbel are made using QQ-, PP-, CDF-plots and histograms.

iv. Although the transformed data might resemble a standard Gumbel distribution, the ACF complemented by simple visualization of the time series data will ascertain whether the development trend has been extracted properly from the transformation.

6.4 Modeling Copulas

As triangle interdependence is extracted in the transformation, the cross dependence should ideally be the only dependence remaining. Hence, the linear and rank correlation measures between LoBs give the cross dependencies. As this application involves three LoBs, i.e. dimensions, a copula that can capture all correlation patterns is preferred, since identical dependence between LoBs would be a substantial generalization of the problem. As previously stated, elliptical copulas provide this property.

Applying Sklar's theorem, a copula may be constructed such that

$$H\left(\tilde{Y}^{(1)}, \tilde{Y}^{(2)}, \tilde{Y}^{(3)}\right) = C_{\Sigma}\left(F(\tilde{Y}^{(1)}), F(\tilde{Y}^{(2)}), F(\tilde{Y}^{(3)})\right) \approx \tag{6.7}$$

$$\approx C_{\Sigma}\left(F(\tilde{Z}), F(\tilde{Z}), F(\tilde{Z})\right)$$

where Σ is the dependence parameter corresponding to copula C and $\tilde{Z} \sim Gumbel(0, 1)$. For validation of the appropriateness of each copula, the Cramér-von Mises goodness of fit test S_nC is used against the empirical joint distribution that is obtained from the three transformed LoBs $\tilde{Y}^{(n)}$. This validation is done using the gofCopula from the copula package in R. The Cramér-von Mises statistics for each copula and its corresponding optimal dependence parameter(s) is then obtained.

Following a simulation of the copula $C_\Sigma(F(\tilde{Z}), F(\tilde{Z}), F(\tilde{Z}))$, a mapping of the simulation to the respective matrices n is performed, such that the dependence parameter Σ has been incorporated between the LoBs. Note that each matrix now corresponds to a completed run-off triangle of generated standard Gumbel observations, where the bottom right part from the diagonal has been filled in. In order to return to the non-stationary distribution, the values are re-transformed such that $\hat{Y}_j^{(n)}$ is obtained from $\tilde{Z}$ by the inverse of the transformation function stated in Definition 3.1. Using $\hat{Y}_j^{(n)}$ and $\tilde{Z}$, the inverse transformation is defined as

$$\hat{Y}_j^{(n)} = \mu^{(n)}(j) + \frac{\sigma^{(n)}(j)}{\gamma^{(n)}} \left(e^{\gamma^{(n)} \tilde{Z}} - 1 \right) \tag{6.8}$$

Following the re-transformation, the estimated payments $\hat{X}^{(n)}$ are obtained after re-weighting corresponding $\hat{Y}^{(n)}$ with $\omega_i^{(n)}$, i.e. $\hat{X}^{(n)} = \hat{Y}^{(n)} \omega_i^{(n)}$. Thus, the estimated future payments are obtained from the lower right side of the now complete run-off triangle.

To replicate the dynamics and uncertainties of the reserves, Monte Carlo simulations (MC) are performed in order to obtain its empirical joint distribution. The Monte Carlo simulations are performed such that new random samples from the standard Gumbel distributions are gererated for each iteration.

6.5 Process Flow Chart

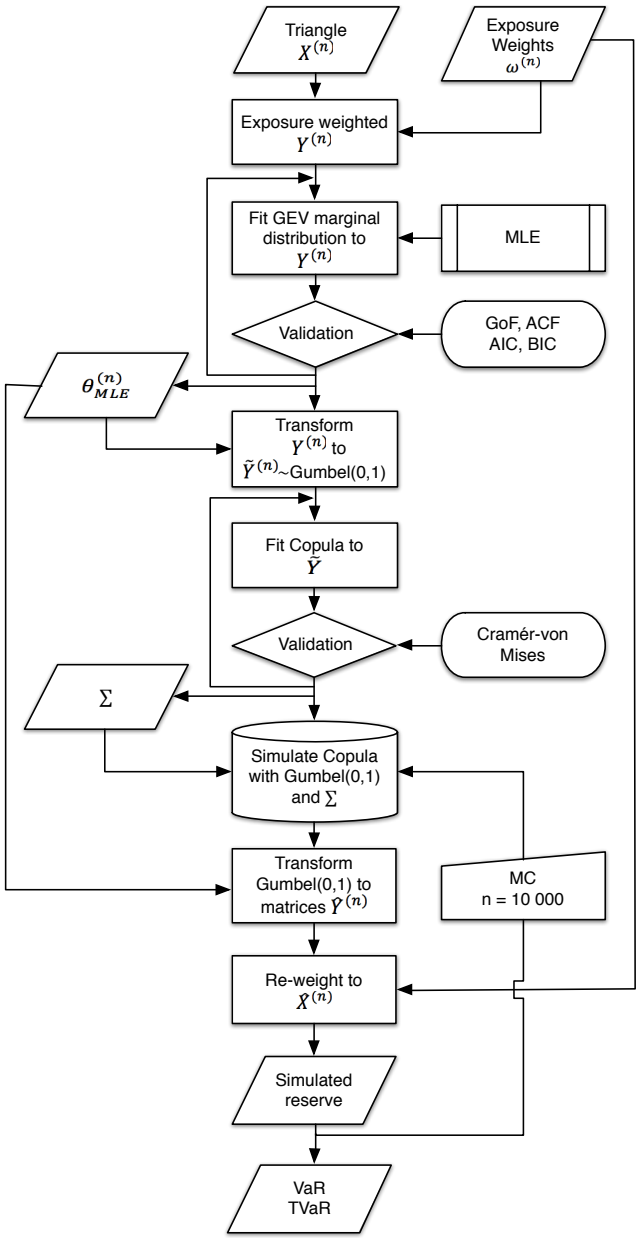

Chapter 7

7 Result

7.1 MLE Model Validation

MLE values are presented in the following three tables for respective LoB. Due to performance issues of constrOptim, for the considerably small data set, when maximizing the log-likelihood function, parameters have been limited to $l, m \leq 3$. In tables 7.1, 7.2 and 7.3, the values for the validation measures are provided[13]. Note that the likelihood ratio values are evaluated in comparison to its preceding model, such that the compared 95 percent chi-squared quantile has one degree of freedom[14]. An improved model for this significance level has been underlined.

Table 7.1 Aviation Model Validation

$Y^{(1)}_{l,m}(j)$	$\ln \mathcal{L}(\bar{\eta}(j), \zeta; \mathbf{Y})$	$-2 \ln \lambda(\mathbf{Y})$	AIC	BIC	$p(D_{K-S})$	iid
$Y_{j,0,0}$	−59.981	−	125.961	136.003	0.401	N
$Y_{j,0,1}$	−58.756	2.450	125.512	138.901	0.495	N
$Y_{j,0,2}$	−58.316	0.880	126.632	143.368	0.0998	N
$Y_{j,0,3}$	−54.024	<u>8.584</u>	120.047	140.130	0.317	N
$Y_{j,1,3}$	−54.024	0.000	122.047	145.477	0.320	N
$Y_{j,2,3}$	4.483	<u>117.014</u>	7.035	33.812	0.0196	Almost
$Y_{j,3,3}$	291.956	<u>574.946</u>	−565.913	−535.789	0.417	Almost

[13] Estimated parameters are provided in Appendix A.4.

[14] The 95 percent chi-square quantile with one degree of freedom is 3.8415

Table 7.2 Marine Model Validation

$Y^{(1)}_{l,m}(j)$	$\ln \mathcal{L}(\bar{\eta}(j), \zeta; \mathbf{Y})$	$-2 \ln \lambda(\mathbf{Y})$	AIC	BIC	$p(D_{K-S})$	iid
$Y_{j,0,0}$	-186.949	$-$	379.897	389.938	0.0149	N
$Y_{j,0,1}$	-183.630	6.638	375.259	388.647	0.0187	N
$Y_{j,0,2}$	-159.461	48.338	328.923	345.658	0.0000	N
$Y_{j,0,3}$	-156.112	6.698	324.225	344.307	0.0000	Almost
$Y_{j,1,3}$	-154.943	2.338	323.887	347.317	0.0000	Almost
$Y_{j,2,3}$	-148.631	12.624	313.262	340.039	0.0276	Almost
$Y_{j,3,3}$	-139.439	18.384	282.112	327.001	0.0871	Almost

Table 7.3 Property Model Validation

$Y^{(1)}_{l,m}(j)$	$\ln \mathcal{L}(\bar{\eta}(j), \zeta; \mathbf{Y})$	$-2 \ln \lambda(\mathbf{Y})$	AIC	BIC	$p(D_{K-S})$	iid
$Y_{j,0,0}$	-77.230	$-$	160.460	170.501	0.0652	N
$Y_{j,0,1}$	-74.136	6.188	156.271	169.660	0.0255	N
$Y_{j,0,2}$	-44.698	58.876	99.396	116.131	0.0000	N
$Y_{j,0,3}$	-2.846	83.704	17.691	37.774	0.0000	Almost
$Y_{j,1,3}$	-3.611	-1.530	21.222	44.652	0.0000	Almost
$Y_{j,2,3}$	4.786	16.794	6.429	33.206	0.0000	Almost
$Y_{j,3,3}$	40.297	71.022	-62.594	-32.470	0.0547	Almost

A visualization of the transformation to $\tilde{Y}^{(n)}$, using the optimal values $\hat{\theta}_{MLE}$ obtained for $l, m = 3$, is provided in Figure 7.1. Row one illustrates the original data and the obtained trend of the location parameter $\mu^{(n)}(j)$ and scale parameter $\sigma^{(n)}(j)$. The resulting transformation is visualized in row two. Ideally a $Gumbel(0, 1)$ distribution is returned, where data is independent. Looking at the third row of Figure 7.1, the plots illustrate a replication of the original data using simulations from the distributions $\hat{Y}^{(n)}_j$.

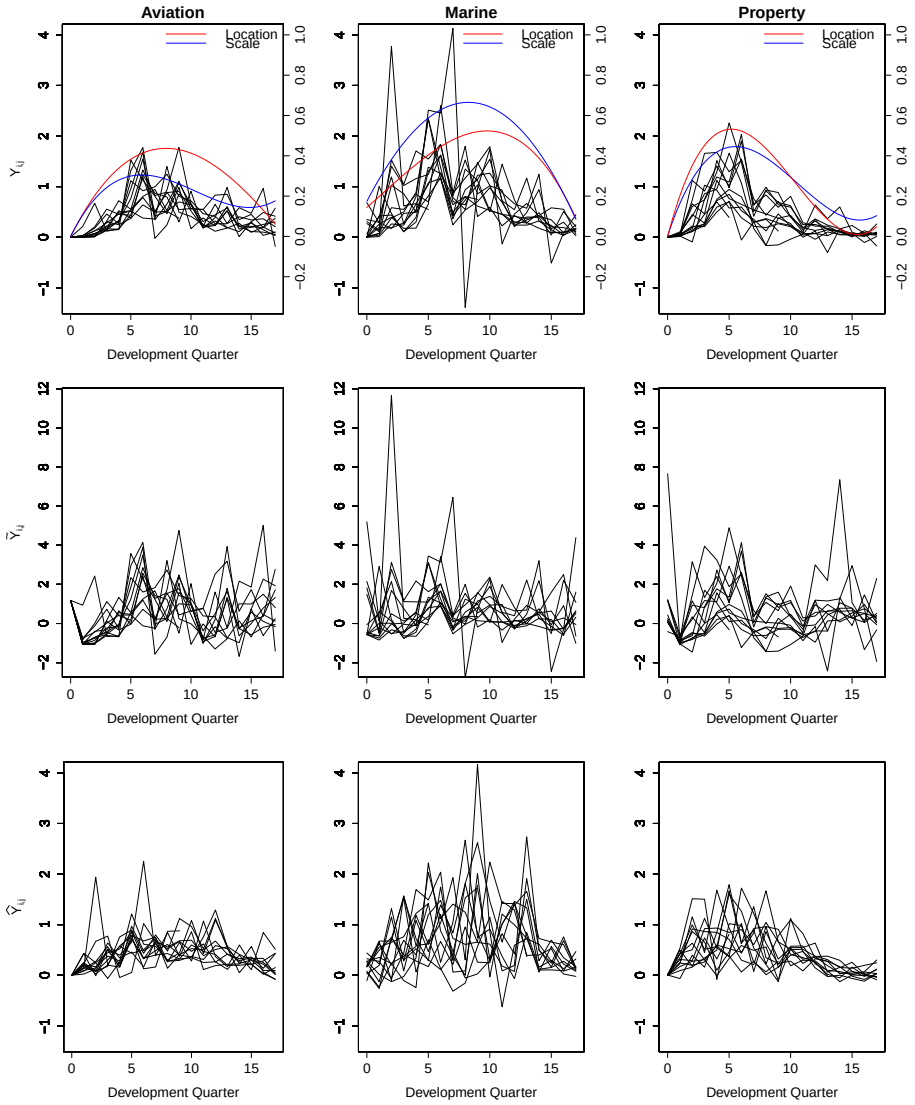

Figure 7.1: *Row 1. The original data* $Y^{(n)}$ *with fitted location and scale parameters* μ_j *and* σ_j*. Row 2. Corresponding transformed data* $\tilde{Y}^{(n)}$*, ideally* $Gumbel(0,1)$*. Row 3. Replication of original data using simulations from* $\hat{Y}_j^{(n)} \sim GEV(\mu^{(n)}(j), \sigma^{(n)}(j), \gamma^{(n)})$*.*

The Kolmogorov-Smirnov goodness of fit reports a p-value indicating that for all transformations $l, m = 3$, their distribution being $Gumbel(0,1)$ cannot be rejected on a 95 percent confidence interval. To further verify the

obtained transformation $\tilde{Y}^{(n)}$, QQ-plots are provided in Figure 7.2.[15] These plots compare the empirical quantiles against the theoretical ones from $Gumbel(0, 1)$.

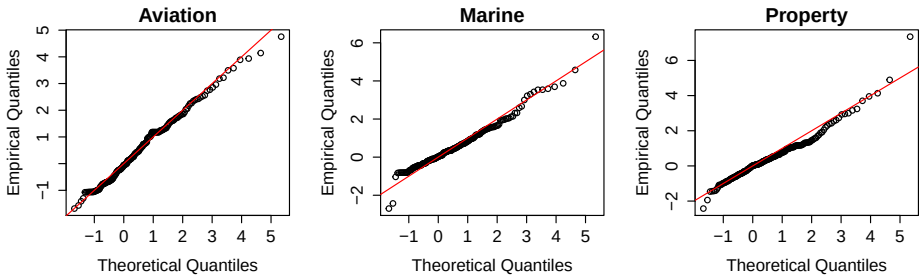

Figure 7.2: *QQ-plots. Empirical quantiles plotted against theoretical quantiles.*

Looking at the transformed data, much of the development dependence appears to be extracted. This is confirmed from the ACF plots in Figure 7.3, where data seems to be independent. Hence, the assumption is made that the transformation using $l, m = 3$ is independent and of the type $\tilde{Y}^{(n)} \sim Gumbel(0, 1)$.

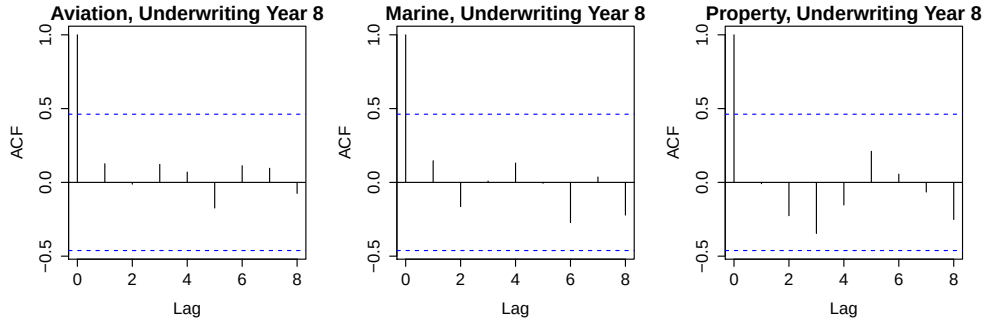

Figure 7.3: *ACF plots for the transformed data $\tilde{Y}^{(n)}$, illustrating horisontal dependence.*

[15] For additional examination of the fit, see validation plots provided in Appendix A.3.

7.2 Copula Modeling

Looking at the cross dependence between LoBs, the resulting values for $\tau_K(\tilde{Y}^{(n)}, \tilde{Y}^{(p)})$ and $\rho_P(\tilde{Y}^{(n)}, \tilde{Y}^{(p)})$ are provided in Table 7.4. The correlation matrix is asymmetric due to the fact that τ_K is presented in the upper right part and ρ_P in the lower left part of the diagonal. One notes a stronger dependence between Property and the other two than between the Marine and Aviation portfolios.

Table 7.4 Dependence Measures

	Aviation	Marine	Property
Aviation	1	0.0600	0.1478
Marine	0.0141	1	0.1500
Property	0.1016	0.1858	1

A summary of estimated values from the gofCopula optimization and validation can be found in Table 7.5, where Σ is ordered as in Table 7.4. Following the dependencies obtained for t-copula, with $\nu = 10.6978$, its corresponding tail dependence is $\bar{\lambda} = \begin{pmatrix} 0.0280 & 0.0533 & 0.0573 \end{pmatrix}$.[16]

Table 7.5 Copula Goodness of Fit

Copula	Σ	S_nC	$p(S_nC)$
Gaussian	$\begin{pmatrix} 1 & 0.094 & 0.230 \\ 0.094 & 1 & 0.233 \\ 0.230 & 0.233 & 1 \end{pmatrix}$	0.3299	0.1294
$t_{10.69}$	$\begin{pmatrix} 1 & 0.084 & 0.218 \\ 0.084 & 1 & 0.234 \\ 0.218 & 0.234 & 1 \end{pmatrix}$	0.3299	0.1773

[16] $\nu = 10.6978$ is the optimal degrees of freedom obtained from fitCopula in R.

7.3 Simulation

From the obtained margins and copula parameters, the simulation is performed using t-copula, Gaussian copula as well as the independent Gaussian copula, where correlations are set to zero, i.e. Σ is the identity matrix. The results from the copula simulations, as well as from the Chain Ladder bootstrap simulation, are summarized in Table 7.6 below. These results are based on running 10 000 Monte Carlo Simulations, as well as 10 000 Chain Ladder bootstrap iterations. The table presents the future estimated losses up to 4.5 years, i.e. the sum of the values in the lower right side of the triangle's diagonal[17].

Table 7.6 Estimated Future Losses per LoB

	Simulated Reserve			Chain Ladder		
LoB	Predicted Loss	Upper Bound	Lower Bound	Predicted Loss	Upper Bound	Lower Bound
Aviation	1,060,000,000	1,757,000,000	513,000,000	1,112,000,000	2,166,000,000	521,000,000
Marine	1,083,000,000	1,981,000,000	401,000,000	524,000,000	1,064,000,000	112,000,000
Property	4,518,000,000	8,666,000,000	1,132,000,000	2,070,000,000	3,322,000,000	772,000,000

Finally aggregated reserve estimates for the standard deviations and risk measures VaR and TVaR, using the appropriate quantiles are provided in Table 7.7.[18]

Table 7.7 Aggregated Estimated Risk Measures

Copula	Standard Deviation	$\text{VaR}_{99.5\%}$	$\text{VaR}_{99.7\%}$	$\text{TVaR}_{99.5\%}$
t	1,072,000,000	9,649,000,000	9,896,000,000	10,130,000,000
Gaussian	1,062,000,000	9,609,000,000	9,802,000,000	9,918,000,000
Independent	1,002,000,000	9,476,000,000	9,680,000,000	9,802,000,000

[17] Due to confidentiality, the values provided in Table 7.6 and 7.7 have been crypted.
[18] The risk measures applied on each LoB respectively are provided in Appendix A.5.

Chapter 8

8 Conclusion and Discussion

When comparing the estimated reserve calculated using the non-stationary distributions against the Chain Ladder bootstrap, one can see in Table 7.6 that they differ, especially for Marine and Property. In both cases the copula approach gives a higher estimated reserve and a substantially higher estimated standard deviation[19]. This is despite the fact that the bootstrap model generally has a high standard deviation, as it takes parameter uncertainty into account.

As previously mentioned, simulations from the non-stationary distributions $\hat{Y}_j^{(n)}$ are illustrated in row three of Figure 7.1. Ideally these replications should resemble the original data $Y^{(n)}$. One generally notes that neither the location nor scale parameter is able to fully adapt to the true dynamics. Especially for Marine and Property the scale parameter appears to be overestimated for many development quarters j. This helps to explain the considerably low p-values obtained for the two LoBs using Kolmogorov-Smirnov goodness of fit test. Preferably, one would hope for significantly higher p-values. To further explore the reasons behind the deviating results, densities of $\hat{Y}_j^{(n)}$ are compared to the actual column mean in Figure 8.1.

As can be seen in Figure 8.1, the densities of the distributions $\hat{Y}_j^{(n)}$ do not fully coincide with the average of corresponding column in $Y_j^{(n)}$. A poorer match is seen for Marine and Property as the densities are not in line with the observed average, i.e. the vertical lines. This is better observed in Table 8.1, where corresponding means and standard deviations are compared directly. When applying weights to obtain the true estimates $\hat{X}^{(n)}$, the discrepancies are then magnified based on the size of the exposure weights $\omega_i^{(n)}$. Additionally, the appearance of the probability density functions for earlier

[19]The standard deviations for each LoB are presented in Appendix A.5.

development quarters are very wide, and Table 8.1 confirms an overestimated scale factor for some columns[20]. Hence, it can be concluded that the obtained cubic dynamics of the location and scale parameter do not suffice as a parameter choice, at least not Marine and Property.

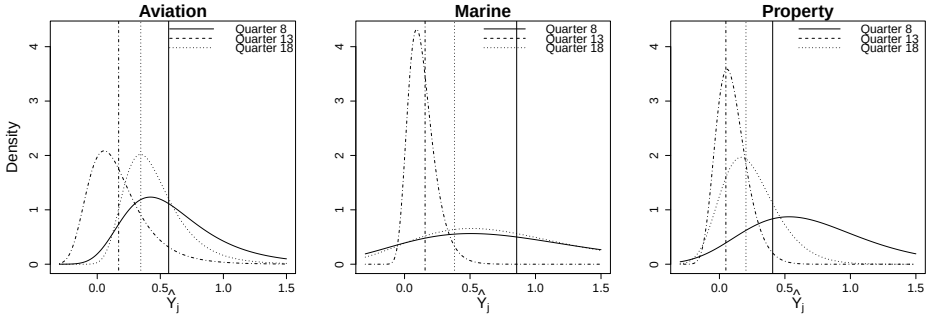

Figure 8.1: *Density plots for* $\hat{Y}_j^{(n)}$, $j = (7, 12, 17)$ *and the corresponding average of* $Y_j^{(n)}$, *marked as a vertical line.*

Table 8.1 Estimated Fit versus Original Data

	$\hat{Y}_j^{(n)}$		$Y_j^{(n)}$	
LoB_{column}	Mean	Standard Deviation	Mean	Standard Deviation
$Aviation_7$	0.614	0.401	0.566	0.299
$Aviation_{12}$	0.461	0.245	0.345	0.203
$Aviation_{17}$	0.167	0.238	0.170	0.199
$Marine_7$	0.832	0.797	0.856	1.006
$Marine_{12}$	0.791	0.684	0.381	0.181
$Marine_{17}$	0.135	0.104	0.157	0.106
$Property_7$	0.696	0.487	0.407	0.194
$Property_{12}$	0.239	0.216	0.203	0.181
$Property_{17}$	0.098	0.118	0.049	0.093

[20]The overestimated scale factor for Marine and Property is reflected as a large standard deviation in Appendix A.5.

As is noted in the second row of Figure 7.1, the trend for the LoB was not fully extracted. The optimization method constrOptim struggled to fit nine parameters to the limited amount of data. If provided with an alternative optimization method, performance may improve, resulting in better transformations.

Regarding the data applied in this thesis, the purpose of introducing development quarter intervals was to get more accurate information of the dynamics of the data and increasing the amount of data at hand. While serving this purpose, the non-linearity of the data becomes more complex, which complicates parameter estimation in MLE.

An additional complicating factor is the nature of reinsurance data. The largest occurred losses have been extracted from the data since this would offset modeling of "regular" claim data. Despite this extraction, the sizes and development of reinsurance claims differ from ordinary insurance claims, with data having more outliers and generally longer maturities. Therefore, the marginal fits might improve if applied to more predictive data.

The more general problem for run-off triangles concerns the limitation of data. As the used data has at most $I = 13$ values in each column (even less for higher columns), the uncertainty is large, thus resulting in high variance estimates. In order to better cope with this issue, one might consider increasing granularity, for instance by replacing underwriting/accident years with quarterly data. However, for underwriting quarters, the issues regarding exposure weighting and vertical dependence will become more prominent, since generally a majority of contracts are signed in the beginning of the year. Another solution is to include earlier accident years. However, one must consider the tradeoff between more data and the decreasing relevance of old data.

Taking the marginal fits $\hat{Y}^{(n)}$ as given, the impact from the choice of copula is seen in the reserve amounts, generating risk measures that vary between one and three percent depending on the copula. A graphical representation of the joint reserve for Marine and Property is displayed in Figure 8.2.

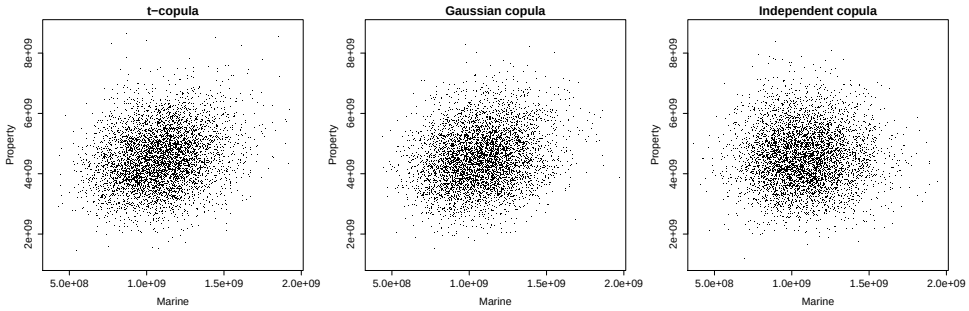

Figure 8.2: *Reserve simulations for Marine and Property.*

Due to the positive dependence that t and Gaussian copula exhibit, larger reserve estimates are generally obtained, as the diversification effects are not as large as for the independent case. Additionally, note the difference in properties for the t-copula and the Gaussian copula previously demonstrated in Figure 4.1. The higher standard deviation comes from the effect of t-copula having more outliers. One also notes more extreme values in the tails for the t-copula, caused by its tail dependence. This property is reflected in the higher VaR and TVaR obtained, and is more prominent for more extreme tail events. This is verified by the marginal increase from $\text{VaR}_{99.5\%}$ to $\text{VaR}_{99.7\%}$, where the t-copula generates an increase by approximately 2.56 percent, whereas the same increase is 2.01 and 2.16 percent for Gaussian copula and independent copula respectively.

The p-value for Cramér-von Mises S_nC reports that the transformations $\tilde{Y}^{(n)}$ coming from an observation of a t-copula is most significant. Although $p(S_nC_{t-copula}) = 0.1773$ is not considered high, it can still be assumed sufficient. One should therefore assume that the joint dynamics of the portfolios behave more in line with the t-copula than with the other two.

For this data, sizes of the LoBs are uneven. The Property portfolio is several times larger than both Aviation and Marine, thus accounting for a large share of the aggregated reserve. Had the portfolios been more equal in terms of size, larger effects from dependencies and choice of copula would have been observed.

8.1 Recommendations

The model applied on the given data cannot be considered sufficient. The reason for this is the non-stationary margins, which are not fully able to adapt to the development of IBNR claims. If better marginal fits can be accomplished, it is a different matter. However, one must consider the model risk and parameter uncertainty which may result in unrealistic estimates.

The model's ties to run-off triangle theory has its pros and cons. It makes it more intuitive for practitioners in the field, but it is bound to the limitations of general run-off triangle theory, such as shortage of data caused by data merging.

Nevertheless, the theoretical approach taken in this thesis is one that can be considered fairly general and applicable for loss reserving. It allows the user to adapt marginal distributions that are free of choice and to choose which marginal parameters to include within $\eta(i, j)$ or ζ. The flexibility of $\eta(i, j)$ provides the ability of being able to account for vertical, horisontal, as well as calendar year dependence, using any type of trend desired. Following the non-stationary marginal distributions, the large collection of copulas and varying cross dependence parameters can be used for various scenario and stress testing, evaluating impacts from dependence and tail dependence. The run-off triangle framework allows estimated reserves to be presented on a calendar year, development year and/or accident year basis.

Appendix A

A Appendix

A.1 Chain Ladder Bootstrap

Assume the initial Chain Ladder approach has been performed according to Section 3.5.1.1 such that the residual run-off triangle is established. The principle of the Chain Ladder bootstrap is then to rearrange the residual run-off triangle randomly, resulting in a similar appearance as in Table A.1, where $r^*_{i,j}$ is denoted as the new residual in position i, j (for instance, $r^*_{1,0} = r_{I-4,2}$ in Table A.1).

Table A.1 Rearranged Residual Triangle

	Development Lag				
Accident Year	0	1	$\cdots$	$J-1$	J
1	$r_{I-4,2}$		$\cdots$	$r_{2,J-6}$	$r_{I-1,1}$
2				$r_{3,J-I-1}$	
		$\ddots$			
$\vdots$	$\vdots$		$\iddots$		
			$r_{1,2}$		
		$\iddots$			
$I-1$	$r_{1,J}$	$r_{i,j}$			
I	$r_{i-3,1}$				

Once rearranging has been made, using (3.4), a new incremental triangle X^* is constructed such that

$$X^*_{i,j} = r^*_{i,j}\sqrt{\hat{C}_{i,j} - \hat{C}_{i,j-1}} + (\hat{C}_{i,j} - \hat{C}_{i,j-1}), \quad i + j \leq J + 1 \tag{A.1}$$

The incremental triangle can easily be reconstructed to a cumulative triangle C^*. Using the previously obtained development factors $\hat{f}_j$, the triangle can be completed and estimated payments can be established. The random resampling as well as the procedure that follows is done a significant number of times, such that an empirical distribution is obtained and reserves can be set.

A.2 Standard Gumbel Transformation

Transforming $X \sim GEV(\mu, \sigma, \gamma)$ to $g(X) = \tilde{X} \sim Gumbel(0, 1)$.

$$P(g(X) \leq x) = P(X \leq g^{-1}(x)) = \exp(-e^{-x})$$

$$\exp\left\{-e^{-x}\right\} = \exp\left\{-\left(1 + \gamma\frac{g^{-1}(x) - \mu}{\sigma}\right)^{-1/\gamma}\right\}$$

$$\Longleftrightarrow$$

$$e^{-x} = \left(1 + \gamma\frac{g^{-1}(x) - \mu}{\sigma}\right)^{-1/\gamma}$$

$$\Longleftrightarrow$$

$$x = \frac{1}{\gamma}\ln\left\{1 + \gamma\frac{g^{-1}(x) - \mu}{\sigma}\right\}$$

A.3 Marginal Validation Plots

The following figures illustrate the CDF, PP and density plots of $\tilde{Y}^{(n)}$ for Aviation, Marine and Property, compared to the theoretical standard Gumbel.

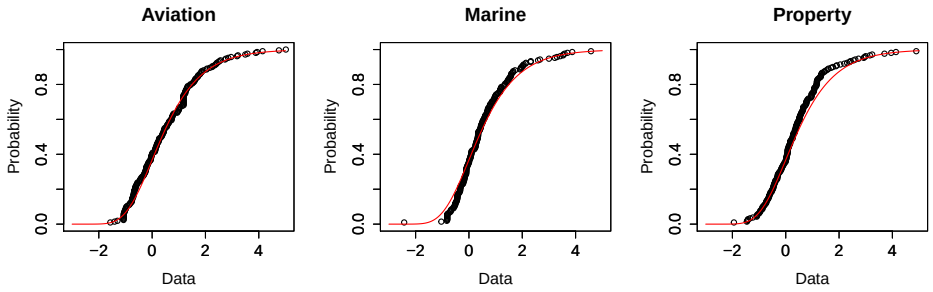

Figure A.1: *Empirical and theoretical CDFs*

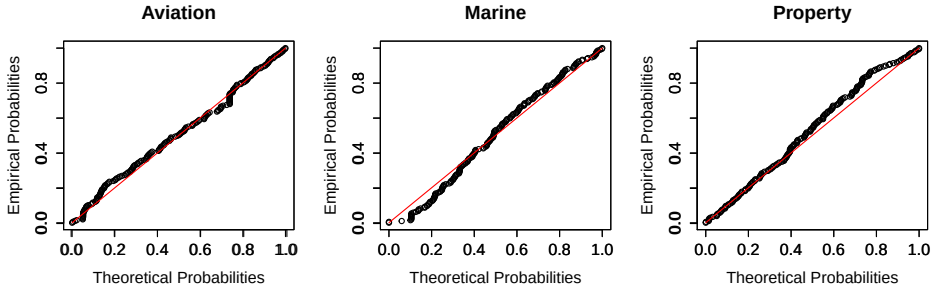

Figure A.2: *PP-plots*

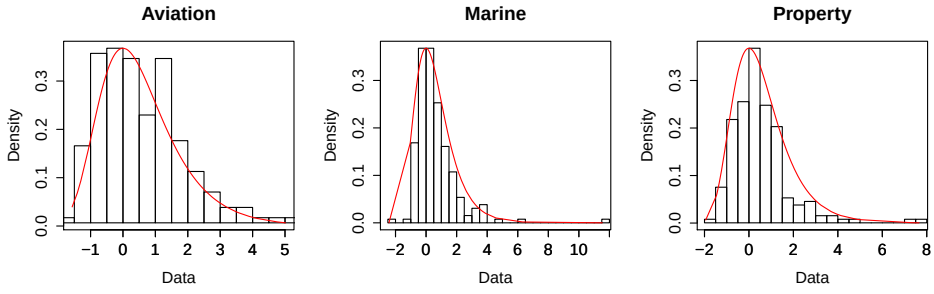

Figure A.3: *Histograms and theoretical densities*

A.4 MLE Parameters

Table A.5 Aviation MLE

$Y^{(1)}_{j,l,m}$	μ_0	μ_1	μ_2	μ_3	σ_0	σ_1	σ_2	σ_3	γ
$Y_{j,0,0}$	0.229	–	–	–	0.248	–	–	–	0.173
$Y_{j,0,1}$	0.242	–	–	–	0.281	−0.0035	–	–	0.133
$Y_{j,0,2}$	0.263	–	–	–	0.327	−0.0197	0.0009	–	0.198
$Y_{j,0,3}$	0.247	–	–	–	0.269	0.0427	−0.0083	0.0003	0.160
$Y_{j,1,3}$	0.246	0.0000	–	–	0.269	0.0428	−0.0083	0.0003	0.159
$Y_{j,2,3}$	−0.103	0.156	$-9.096 \cdot 10^{-3}$	–	0.0618	0.0453	−0.0022	0.0000	$4.310 \cdot 10^{-2}$
$Y_{j,3,3}$	0.0000	0.119	$-9.185 \cdot 10^{-3}$	$1.405 \cdot 10^{-4}$	0.0000	0.190	−0.0141	0.0004	$3.437 \cdot 10^{-2}$

Table A.6 Marine MLE

$Y^{(2)}_{j,l,m}$	μ_0	μ_1	μ_2	μ_3	σ_0	σ_1	σ_2	σ_3	γ
$Y_{j,0,0}$	0.405	–	–	–	0.538	–	–	–	$-6.743 \cdot 10^{-2}$
$Y_{j,0,1}$	0.385	–	–	–	0.631	−0.0119	–	–	$-7.728 \cdot 10^{-2}$
$Y_{j,0,2}$	0.175	–	–	–	0.200	0.121	$-7.515 \cdot 10^{-3}$	–	$-3.335 \cdot 10^{-2}$
$Y_{j,0,3}$	0.171	–	–	–	0.189	0.171	$-1.588 \cdot 10^{-2}$	$3.170 \cdot 10^{-4}$	$-6.257 \cdot 10^{-2}$
$Y_{j,1,3}$	0.231	−0.0045	–	–	0.226	0.184	$-1.863 \cdot 10^{-2}$	$4.330 \cdot 10^{-4}$	$-8.535 \cdot 10^{-2}$
$Y_{j,2,3}$	0.127	0.105	−0.0062	–	0.223	−0.0060	$-1.565 \cdot 10^{-2}$	$-9.307 \cdot 10^{-4}$	$-1.788 \cdot 10^{-2}$
$Y_{j,3,3}$	0.144	0.0535	−0.0010	$-2.545 \cdot 10^{-4}$	0.174	0.117	$-6.826 \cdot 10^{-3}$	$-2.285 \cdot 10^{-5}$	$-4.014 \cdot 10^{-2}$

Table A.7 Property MLE

$Y^{(3)}_{j,l,m}$	μ_0	μ_1	μ_2	μ_3	σ_0	σ_1	σ_2	σ_3	γ
$Y_{j,0,0}$	0.163	–	–	–	0.260	–	–	–	0.2263
$Y_{j,0,1}$	0.132	–	–	–	0.385	−0.0132	–	–	8.7197
$Y_{j,0,2}$	0.0006	–	–	–	0.0020	0.0983	$-5.461 \cdot 10^{-3}$	–	0.1116
$Y_{j,0,3}$	0.0009	–	–	–	0.0034	0.236	$-2.933 \cdot 10^{-2}$	$9.2560 \cdot 10^{-4}$	$-8.659 \cdot 10^{-2}$
$Y_{j,1,3}$	0.000	0.000	–	–	0.0036	0.238	$-2.947 \cdot 10^{-2}$	$9.299 \cdot 10^{-4}$	$-8.959 \cdot 10^{-2}$
$Y_{j,2,3}$	0.006	0.0061	−0.0002	–	0.0032	0.212	$-2.626 \cdot 10^{-2}$	$8.297 \cdot 10^{-4}$	$-6.999 \cdot 10^{-2}$
$Y_{j,3,3}$	−0.0002	0.231	−0.0298	$9.618 \cdot 10^{-4}$	0.0038	0.182	$-2.231 \cdot 10^{-2}$	$7.037 \cdot 10^{-4}$	$9.677 \cdot 10^{-2}$

A.5 Estimated Line of Business Risk Measures

For completeness as well as comparability against the Chain Ladder bootstrap simulation, standard deviations and risk measures are provided separately for each LoB.

Table A.2 Aviation - Estimated Risk Measures

LoB	Standard Deviation	$\text{VaR}_{99.5\%}$	$\text{VaR}_{99.7\%}$	$\text{TVaR}_{99.5\%}$
t	147,000,000	1,477,000,000	1,511,000,000	1,536,000,000
Gaussian	147,000,000	1,484,000,000	1,509,000,000	1,541,000,000
Independent	147,000,000	1,480,000,000	1,512,000,000	1,535,000,000
Chain Ladder	181,000,000	1,725,000,000	1,781,000,000	1,829,000,000

Table A.3 Marine - Estimated Risk Measures

LoB	Standard Deviation	$\text{VaR}_{99.5\%}$	$\text{VaR}_{99.7\%}$	$\text{TVaR}_{99.5\%}$
t	219,000,000	1,695,000,000	1,748,000,000	1,787,000,000
Gaussian	218,000,000	1,690,000,000	1,745,000,000	1,779,000,000
Independent	219,000,000	1,695,000,000	1,730,000,000	1,774,000,000
Chain Ladder	108,000,000	874,000,000	911,000,000	925,000,000

Table A.4 Property - Estimated Risk Measures

LoB	Standard Deviation	$\text{VaR}_{99.5\%}$	$\text{VaR}_{99.7\%}$	$\text{TVaR}_{99.5\%}$
t	967,000,000	7,268,000,000	7,478,000,000	7,658,000,000
Gaussian	959,000,000	7,151,000,000	7,319,000,000	7,502,000,000
Independent	968,000,000	7,162,000,000	7,404,000,000	7,530,000,000
Chain Ladder	286,000,000	2,834,000,000	2,881,000,000	2,940,000,000

References

[1] R. L. Bornhuetter and R. E. Ferguson. The Actuary and IBNR. *Proceedings of the Casualty Actuarial Society 59*, (112), 1972.

[2] Peng Shi and Edward W. Frees. Dependent Loss Reserving Using Copulas. 2010.

[3] Piet de Jong. Modeling dependence between loss triangles. *Nort American Actuarial Journal 16.1*, 2012.

[4] H Cosette A Abdallah, J-P Boucher. Modeling dependence between loss triangles using Hierarchical Archimedean Copulas Modeling dependence between loss triangles using Hierarchical Archimedean Copulas Modeling dependence between loss triangles using Hierarchial Archimedean Copulas. 2013.

[5] A Sandström. Solvency - a historical review and som pragmatic solutions. 2007.

[6] Dr H Müller. Solvency of Insurance Undertakings. 1997. Conference of insurance supervisory services of the member states of the European Union.

[7] N. Kumar P. ChandraShekhar and S. R. Warrier. Journey of Insurer Solvency regulations - 2007 and beyond. 2007.

[8] Solvency II Implementaion Date. http://www.lloyds.com/the-market/operating-at-lloyds/solvency-ii/legislative-developments/solvency-ii-implementation-date, May 2014.

[9] Financial Services Authority, UK. http://www.fsa.gov.uk/about/what/international/solvency/policy/european, May 2014.

[10] Glenn Meyers. The Technical Provisions in Solvency II What EU Insurers Could Do if They Had Schedule P. 2010.

[11] Rüdiger Frey Alexander J. McNeil and Paul Embrechts. *Quantitative risk management: concepts, techniques and tools*. Princeton University Press, 2005.

[12] J.F. Wahlin S. Desmedt. On the Subadditivity of Tail-Value at Risk: An Investigation with Copulas. *Variance*, 2(2), 2008.

[13] Björn Weindorfer. A practical guide to the use of the chain-ladder method for determining technical prosisions for outstanding reported claims in non-life insurance. Technical Report 77, University of Applied Sciences bfi Vienna, 2012.

[14] Guy Carpenter. http://www.guycarp.com/content/guycarp/en/home/the-company/media-resources/glossary/a.html, May 2014.

[15] Marco A. Ramírez Corzo Enrique de Alba. Bayesian Claims Reserving When There Are Negative Values in the Runoff Triangle. In *40 th. Actuarial Research Conference, ITAM, Mexico*, August 2005.

[16] James R. Garven Neil A. Doherty. Insurance cycles: Interest rates and the capacity constraint model. *The Journal of Business*, 68(3):383, 1995.

[17] Debarati Guha-Sapir Jennifer Leaning. Natural disasters, armed conflict, and public health. *New England Journal of Medicine*, 369(19):1836–1842, 2013.

[18] Michal Pešta. Bootstrap methods in reserving. In *Actuarial Seminar, Prague*, December 2011.

[19] Paul R. Hussian Paul J. Struzzieri. Using Best Practice to Determine a Best Reserve Estimate. *CAS Forum*, Fall 1998.

[20] Stuart Coles. *An introduction to statistical modeling of extreme values*. Springer, 2001.

[21] Fabrizio Durante Piotr Jaworski. *Copula Theory and Its Applications*. Springer, 2010.

[22] Roger B. Nelsen. *An introduction to Copulas*. Springer, second edition, 2006.

[23] Alireza Bayestehtashk and Izhak Shafran. Parsimonious Multivariate Copula Model for Density Estimation. *ICASSP*, 2013.

[24] Stefano Demarta and Alexander J. Mcneil. The t copula and related copulas. *International Statistical Review*, 73:111–129, 2005.

[25] Kenneth P. Burnham and David Raymond Anderson. *Model selection and multimodel inference: a practical information-theoretic approach*. Springer, 2nd edition, 2002.

[26] Andreas Jakobsson. *An Introduction to Time Series Modeling*. Studentlitteratur, 2013.

[27] Daniel Peña Ana Justel and Rubén Zamar. A Multivariate Kolmogorov-Smirnov Test of Goodness of Fit. 1994.

[28] B. Rémillard C. Genest and D.. Beaudoin. Goodness-of-fit tests for copulas: A review and a power study. *Insurance: Mathematics and Economics*, 44(2):199–213, 2009.

[29] Lasse Klingberg. Chief actuary. Sirius International, April 2014.